bioRxiv preprint doi: https://doi.org/10.1101/848705; this version posted November 20, 2019. The copyright holder for this preprint (which was not certified by peer review) is the author/funder, who has granted bioRxiv a license to display the preprint in perpetuity. It is made available under aCC-BY-NC-ND 4.0 International license.

Characterisation of the *ERF102* to *ERF105* genes of *Arabidopsis thaliana* and their role in the response to cold stress

Sylvia Illgen[1], Stefanie Zintl[1], Ellen Zuther[2], Dirk K. Hincha[2], Thomas Schmülling[1]

[1]*Institute of Biology/Applied Genetics, Dahlem Centre of Plant Sciences (DCPS), Freie Universität Berlin, D-14195 Berlin, Germany*

[2]*Max-Planck-Institute of Molecular Plant Physiology, D-14476 Potsdam, Germany*

Corresponding author:

Thomas Schmülling

Institute of Biology/Applied Genetics

Dahlem Centre of Plant Sciences (DCPS)

Freie Universität Berlin

Albrecht-Thaer-Weg 6

D-14195 Berlin, Germany

Email: tschmue@zedat.fu-berlin.de

bioRxiv preprint doi: https://doi.org/10.1101/848705; this version posted November 20, 2019. The copyright holder for this preprint (which was not certified by peer review) is the author/funder, who has granted bioRxiv a license to display the preprint in perpetuity. It is made available under aCC-BY-NC-ND 4.0 International license.

Abstract

The *ETHYLENE RESPONSE FACTOR* (*ERF*) genes of *Arabidopsis thaliana* form a large family encoding plant-specific transcription factors. Here, we characterise the four phylogenetically closely related *ERF102/ERF5*, *ERF103/ERF6*, *ERF104* and *ERF105* genes. Expression analyses revealed that these four genes are similarly regulated by different hormones and abiotic stresses. Analyses of tissue-specific expression using *promoter:GUS* reporter lines revealed their predominant expression in root tissues including the root meristem (*ERF103*), the quiescent center (*ERF104*) and the root vasculature (all). All GFP-ERF fusion proteins were nuclear-localised. The analysis of insertional mutants, amiRNA lines and *35S:ERF* overexpressing transgenic lines indicated that *ERF102* to *ERF105* have only a limited impact on regulating shoot and root growth. Previous work had shown a role for ERF105 in the cold stress response. Here, measurement of electrolyte leakage to determine leaf freezing tolerance and expression analyses of cold-responsive genes revealed that the combined activity of ERF102 and ERF103 is also required for a full cold acclimation response likely involving the CBF regulon. Together, these results suggest a common function of these *ERF* genes in regulating root architecture and the response to cold stress.

Key-words: Arabidopsis thaliana, cold acclimation, *ETHYLENE RESPONSE FACTOR* genes, freezing tolerance, root architecture, transcription factor

bioRxiv preprint doi: https://doi.org/10.1101/848705; this version posted November 20, 2019. The copyright holder for this preprint (which was not certified by peer review) is the author/funder, who has granted bioRxiv a license to display the preprint in perpetuity. It is made available under aCC-BY-NC-ND 4.0 International license.

INTRODUCTION

The *ERF* genes encode plant-specific transcription factors forming a large gene family with 122 members in *Arabidopsis thaliana* (Nakano, Suzuki, Fujimura & Shinshi, 2006). The ERF transcription factors are members of the APETALA2/ETHYLENE RESPONSE FACTOR (AP2/ERF) superfamily, which also contains the AP2 and RAV families and which is defined by the AP2/ERF DNA-binding domain (Riechmann *et al*., 2000). This domain is about 60 amino acids long and forms an interface of three antiparallel β-strands and one α-helix (Ohme-Takagi & Shinshi, 1995). The β-strands bind to an 11 bp consensus sequence (5'-TAAGAGCCGCC-3'), the GCC-Box, in the major groove of the DNA double helix (Hao, Ohme-Takagi & Sarai, 1998). ERF transcription factors are involved in the regulation of numerous developmental processes (Riechmann & Meyerowitz, 1998) and they are important for the response to various biotic and abiotic stresses including cold (Agarwal, Agarwal, Reddy & Sopory, 2006b; Kizis, Lumbreras & Pages, 2001; Srivastava & Kumar 2019; Xie, Nolan, Jiang & Yin, 2019).

Previously, we identified four phylogenetically closely related *ERF* genes with similar transcriptional responses to cytokinin (Brenner, Romanov, Köllmer, Bürkle & Schmülling, 2005). These genes, *ERF102* (AT5G47230; known as *ERF5*), *ERF103* (AT4G17490; identical to *ERF6*), *ERF104* (AT5G61600) and *ERF105* (AT5G51190) are members of group IXb of the ERF family (Nakano *et al*., 2006). Expression of *ERF102* to *ERF105* is regulated by cold and different cold stress-related hormones, and it was demonstrated that *ERF105* has a function in the freezing tolerance and cold acclimation of *Arabidopsis* (Bolt, Zuther, Zintl, Hincha & Schmülling, 2017). All four *ERF* genes are also involved in the response to other stresses. *ERF102* and *ERF103* regulate leaf growth inhibition upon mild osmotic stress (Dubois *et al*., 2013, 2015) and *ERF103* additionally regulates oxidative stress responses (Sewelam *et al*., 2013). *ERF103*, *ERF104* and *ERF105* are involved in the fast retrograde signalling response and the acclimation response to high light (Moore, Vogel & Dietz, 2014; Vogel *et al*., 2014). Further studies have shown that *ERF102* to *ERF105* play a role in plant immunity (Bethke *et al*.,

bioRxiv preprint doi: https://doi.org/10.1101/848705; this version posted November 20, 2019. The copyright holder for this preprint (which was not certified by peer review) is the author/funder, who has granted bioRxiv a license to display the preprint in perpetuity. It is made available under aCC-BY-NC-ND 4.0 International license.

2009; Cao *et al*., 2019; Mase *et al*., 2013; Meng *et al*., 2013; Moffat *et al*., 2012; Son *et al*., 2012). Thus, ERF102 to ERF105 match the profile of other ERF transcription factors designated as a regulatory hub integrating hormone signalling in the plant response to abiotic stresses (Müller & Munné-Bosch, 2015).

The close phylogenetic relationship among the four *ERF* genes and the similarity of their transcriptional responses to different cues suggested that they share some common functions in response to cold. Cold stress adversely affects plant growth and development and several pathways to respond to cold stress have been described. Plants from temperate and boreal climates have evolved mechanisms to acquire freezing tolerance through cold acclimation, a process in which upon exposure to low non-freezing temperatures the ability to survive freezing temperatures increases (Xin & Browse, 2000). A central cold signalling pathway is the CBF (*C-REPEAT-BINDING FACTOR/DEHYDRATION-RESPONSE ELEMENT-BINDING PROTEIN*) regulon. The *CBF1* (*DREB1b*), *CBF2* (*DREB1c*) and *CBF3* (*DREB1a*) genes are the central regulatory elements of this regulon (Chinnusamy, Zhu & Zhu, 2007; Liu *et al*., 1998). The INDUCER OF C-REPEAT-BINDING FACTOR EXPRESSION 1 (ICE1), a MYC-type bHLH (basic helix-loop-helix) transcription factor, is post-translationally activated in response to cold (Chinnusamy *et al.*, 2003; Ding *et al*., 2015; Li *et al*., 2017; Miura *et al.*, 2007). ICE1 in turn activates the transcription of the *CBF3* gene (Chinnusamy *et al*., 2003). Besides ICE1, expression of the cold-regulated *CBF* genes is positively controlled by several other transcription factors including ICE2 and CALMODULIN-BINDING TRANSCRIPTION ACTIVATOR 3 (CAMTA3) (Doherty, Van Buskirk, Myers & Thomashow, 2009; Fursova, Pogorelko & Tarasov, 2009). Negative regulators of the CBF regulon are, for instance, the C2H2 zinc finger transcription factor ZAT12 (Vogel, Zarka, Van Buskirk, Fowler & Thomashow, 2005) and MYB15 (Agarwal *et al*., 2006a). MYB15 is in turn negatively regulated by ICE1 (Agarwal *et al*., 2006a) and phosphorylation of MYB15 by MPK6 reduces its affinity to bind to the *CBF3* promoter (Kim *et al*., 2017). The CBF proteins regulate the expression of the *COLD-*

bioRxiv preprint doi: https://doi.org/10.1101/848705; this version posted November 20, 2019. The copyright holder for this preprint (which was not certified by peer review) is the author/funder, who has granted bioRxiv a license to display the preprint in perpetuity. It is made available under aCC-BY-NC-ND 4.0 International license.

REGULATED (*COR*) genes and physiological responses (e.g. accumulation of cryoprotective compounds, modification of cellular structures) that together confer cold acclimation (Thomashow, 1999; Yamaguchi-Shinozaki & Shinozaki, 2006). Transcriptomic analyses of the CBF regulon has revealed that only part (~11%) of the cold-responsive genes is under control of the CBF regulon (Park *et al*., 2015), which was confirmed by gene expression analysis in *cfb* triple mutants (Jia *et al*., 2016; Zhao, Zhang, Xie, Si, Li & Zhu, 2016). It was concluded that only about one-third of the increase in freezing tolerance that occurs in response to low temperature is dependent on the CBF regulon (Park *et al*., 2015). Together, this suggests that an extensive regulatory network involving numerous transcription factors in addition to the best known CBF core regulators governs the response to cold.

We previously identified the *ERF105* gene of *Arabidopsis* as an important factor for *Arabidopsis* freezing tolerance and cold acclimation (Bolt *et al*., 2017). The strongly reduced expression of cold-responsive genes in *ERF105* mutants upon cold acclimation suggests that its action is linked to the CBF regulon. Also the expression of three closely related transcription factor genes, *ERF102*, *ERF103* and *ERF104*, is induced by cold (Bolt *et al*., 2017; Lee, Henderson & Zhua, 2005; Park *et al*., 2015; Vogel *et al*., 2005). It is therefore possible that these transcription factors have a function in the response to cold stress. Here, we have extended our analysis of the *ERF105* gene family. We provide additional transcript data supporting a similar response profile of the *ERF105* family members and show the tissue-specific expressions of *pERF102:GUS* to *pERF104:GUS* as well as the subcellular localisations of GFP-ERF102 to GFP-ERF104 fusion proteins. Single and combined loss-of-function mutants and lines overexpressing single *ERF* genes were analysed for their growth characteristics and cold stress response and reveal partial functional redundancy of the members of this transcription factor subfamily.

MATERIAL AND METHODS

bioRxiv preprint doi: https://doi.org/10.1101/848705; this version posted November 20, 2019. The copyright holder for this preprint (which was not certified by peer review) is the author/funder, who has granted bioRxiv a license to display the preprint in perpetuity. It is made available under aCC-BY-NC-ND 4.0 International license.

Plant material

Arabidopsis thaliana accession Col-0 was used as wild type. The *erf105* mutant, *ERF105* overexpressing lines, *pERF105:GUS* lines, complementation lines of *erf105,* as well as 35S:ami104 and 35S:ami104/105 lines have been described previously (Bolt *et al*., 2017). The T-DNA insertion line *erf102* (SAIL_46_C02) was obtained from the Nottingham Arabidopsis Stock Centre (NASC). After selection of homozygous plants, the location of the T-DNA insertion was verified by sequencing and plants were backcrossed twice with Col-0 to eliminate possible multiple insertions and other background mutations. Complementation of the *erf102* phenotype was tested by introgressing ERF102ox-1 and ERF102ox-2 into the *erf102* background. To generate lines overexpressing *ERF102* to *ERF104*, the genomic coding sequences of *ERF102* to *ERF104* were amplified by PCR, cloned into pDONR221 (Invitrogen, Carlsbad, USA) by using the Gateway cloning system and transferred subsequently into vector pK7WGF2 (Karimi, Depicker & Hilson, 2007b). To generate *pERF102:GUS* to *pERF104:GUS* reporter genes, the promoter regions of the *ERF* genes (~2 kb upstream of the start codon) were amplified by PCR and cloned into pDONR P4-P1R (Invitrogen). To generate the binary destination vectors, the pDONR P4-P1R constructs with the *ERF* promoters and the Gateway entry clone pEN-L1-SI-L2 (Karimi, Bleys, Vanderhaeghen & Hilson, 2007a) harboring the *GUS* reporter gene were then combined into the destination vector pK7m24GW,3 using MultiSite Gateway (Karimi, De Meyer & Hilson, 2005). Artificial microRNA (amiRNA) was used to generate lines with a reduced *ERF103* expression (Schwab, Ossowski, Riester, Warthmann & Weigel, 2006). amiRNAs directed against *ERF104* and *ERF105* were described (Bolt *et al*., 2017). The amiRNA sequence targeting *ERF103* was 5′-TAACGTCGTAACTTTCCCCCG-3′. The sequence was selected and the expression construct was made using the Web MicroRNA Designer (WMD3) and the protocol available under http://wmd3.weigelworld.org. The amiRNA precursor was cloned into pDONR221 (Invitrogen) and subsequently into pH2GW7 (Karimi *et al*., 2007b) harboring the cauliflower mosaic virus (CaMV) *35S* promoter to yield 35S:ami103. All primers

bioRxiv preprint doi: https://doi.org/10.1101/848705; this version posted November 20, 2019. The copyright holder for this preprint (which was not certified by peer review) is the author/funder, who has granted bioRxiv a license to display the preprint in perpetuity. It is made available under aCC-BY-NC-ND 4.0 International license.

used for cloning are listed in Table S1. The binary constructs were transformed into Col-0 plants by *Agrobacterium tumefaciens* (GV3101:pMP90) using the floral dip method as described by Davis, Hall, Millar, Darrah & Davis (2009). Higher order mutants with reduced expression of *ERF* genes were generated by crossing amiRNA lines with T-DNA insertion lines.

Growth conditions, hormone and stress treatment

For hormone and stress treatments, plants were grown *in vitro* under long day (LD) conditions (16 h light/8 h dark) and 21 °C in half strength liquid Murashige and Skoog (MS) medium (for hormone treatment) or on solid MS medium (for stress treatment), in each case containing 0.1 % sucrose (Murashige & Skoog, 1962). Eleven days after germination (DAG), hormonal treatments were performed by adding the respective hormone to the liquid medium. Seedlings grown on solid medium were exposed to different stress treatments eleven DAG, including heat treatment at 42 °C in darkness, high light stress (1000 µmol m^{-2} s^{-1}) instead of standard light (100–150 µmol m^{-2} s^{-1}), oxidative stress by spraying seedlings with 500 mM H_2O_2, drought stress by transferring seedlings to dry filter paper, or salt/osmotic stress by transplanting seedlings to MS medium including 200 mM NaCl or 200 mM mannitol, respectively, for different time periods. Control plants were treated with the respective control conditions, which were the respective mock solution in the hormone experiment, 21 °C in the heat stress experiment, standard light conditions in the high light experiment, spraying with mock solution in the oxidative stress experiment and transferring to moist filter paper in the drought experiment, or mock medium in the salt and osmotic stress experiment.

For the analysis of growth and developmental parameters, plants were grown on soil in the greenhouse under LD conditions (16 h light/8 h dark) at a light intensity of 130–160 µmol m^{-2} s^{-1} and 21 °C. Fourteen, 21, 28, and 35 DAG rosette diameter and shoot height were determined. Furthermore, the flowering time, defined as opening of the first flower, was recorded. Leaf senescence was recorded based on visual inspection of the oldest leaves turning yellow.

bioRxiv preprint doi: https://doi.org/10.1101/848705; this version posted November 20, 2019. The copyright holder for this preprint (which was not certified by peer review) is the author/funder, who has granted bioRxiv a license to display the preprint in perpetuity. It is made available under aCC-BY-NC-ND 4.0 International license.

For analysis of roots, plants were grown *in vitro* in vertically placed square petri dishes on half strength MS medium containing 10 g L^{-1} phytagel. The elongation of the primary root was determined from digital images between four and ten DAG using the software ImageJ (Abràmoff, Magalhaes & Ram, 2004). The number of lateral roots was determined ten DAG from the same images.

For electrolyte leakage experiments, plants were grown for two weeks under SD conditions and then for four weeks under LD conditions at 200 µmol m^{-2} s^{-1} and 20 °C during the day, 18 °C during the night (non-acclimated plants). For cold acclimation, plants were transferred to a cold chamber and cultivated under LD (90 µmol m^{-2} s^{-1}) at 4 °C for additional 14 days.

RNA analysis

Total RNA was extracted from tissues (seedlings in Fig. 2; leaves from six-week-old plants in Figure 6 and Figure S3) using the NucleoSpin RNA Plant Kit (Macherey & Nagel, Düren, Germany) according to the manufacturer's instructions, including an on-column DNase digestion. As a control, quantitative real-time PCR (qRT-PCR) measurements using intron-specific primers for AT5G65080 were performed to confirm the absence of genomic DNA contamination (Zuther, Schulz, Childs & Hincha, 2012). For RT-PCR, 500 ng RNA were reverse transcribed using the QIAGEN OneStep RT-PCR Kit according to the manufacturer's information (Qiagen, Hilden, Germany). The sequences of primers were as follows: *Actin2*-F, 5′-TACAACGAGCTTCGTGTTGC-3′; *Actin2*-R, 5′-GATTGATCCTCCGATCCAGA-3′; *ERF102*-F, 5′-CTGCACTTTGGTTCATCGAG-3′; *ERF102*-R, 5′-GAGATAACGGCGACAGAAGC-3′. For qRT-PCR analyses, 1 µg RNA was transcribed into cDNA by SuperScript III Reverse Transcriptase (Invitrogen) according to the manufacturer's instructions using a combination of oligo(dT) primers and random hexamers. qRT-PCR analyses were performed as previously described by Bolt *et al*. (2017). Four biological replicates

bioRxiv preprint doi: https://doi.org/10.1101/848705; this version posted November 20, 2019. The copyright holder for this preprint (which was not certified by peer review) is the author/funder, who has granted bioRxiv a license to display the preprint in perpetuity. It is made available under aCC-BY-NC-ND 4.0 International license.

were used and each qRT-PCR experiment was performed twice. In all cases both experiments yielded similar results and one result is shown exemplarily.

GUS staining and microscopy

Histochemical analysis to detect GUS reporter enzyme activity was performed as described by Jefferson, Kavanagh & Bevan (1987) with some modifications as described by Bolt *et al.* (2017). GUS analyses were carried out with two or three independent *pERF:GUS* lines for each of the constructs and identical expression patterns were seen. The histochemical analyses were repeated several times with plants of different age.

Transient gene expression in *Nicotiana benthamiana* and confocal laser scanning microscopy

Subcellular localisation of GFP fused to ERF proteins was done in leaves of 6-week-old *N. benthamiana* according to Sparkes, Runions, Kearns & Hawes (2006) with the equipment described by Bolt *et al.* (2017).

Electrolyte leakage

Electrolyte leakage was determined with detached leaves over a temperature range from -1 to -16 °C for non-acclimated plants and from -2 to -22 °C for cold acclimated plants, cooled at a rate of 4 °C h^{-1} as described in detail in Thalhammer, Hincha & Zuther (2014). Four technical replicates were analysed for each temperature point, and for each of these replicates leaves from three different plants were pooled. The temperature of 50 % electrolyte leakage (LT_{50}) was calculated as the log EC50 value of sigmoidal curves fitted to the leakage values using the software GraphPad Prism3 (GraphPad Software, Inc., La Jolla, USA).

Statistical analyses

bioRxiv preprint doi: https://doi.org/10.1101/848705; this version posted November 20, 2019. The copyright holder for this preprint (which was not certified by peer review) is the author/funder, who has granted bioRxiv a license to display the preprint in perpetuity. It is made available under aCC-BY-NC-ND 4.0 International license.

Every experiment was conducted at least twice. Figures show data of a single experiment that is representative of two or three experiments showing similar results. Data are presented as the mean ± standard error. Statistical analyses were performed using SAS or GraphPad Instat Software (one-way ANOVA or two-way repeated measures ANOVA with Tukey's post hoc test). Normality and homogeneity of variance were tested using the Shapiro-Wilk and Levene tests (Neter, Kutner, Nachtsheim & Wasserman, 1996). In order to meet the assumptions, data sets were transformed using log or square-root transformation. If assumptions were not met, a nonparametric Kruskal-Wallis test was carried out followed by a Mann-Whitney test to perform a pairwise comparison.

RESULTS

Phylogenetic analysis and description of the ERF102 to ERF105 proteins of *Arabidopsis thaliana*

According to 'The *Arabidopsis* Information Resource' (TAIR) (Huala *et al*., 2001), *ERF102* to *ERF105* are relatively small, intronless genes with coding regions for proteins containing 300 (ERF102), 282 (ERF103), 241 (ERF104) and 221 (ERF105) amino acids. Like all AP2/ERF transcription factors they possess the characteristic AP2/ERF domain and are the only proteins in group IX with one (ERF102 and ERF103) or two (ERF104 and ERF105) putative phosphorylation sites (Nakano *et al*., 2006). Moreover, ERF102 to ERF105 possess acidic regions that might function as transcriptional activation domains (Fujimoto, Ohta, Usui, Shinshi & Ohme-Takagi, 2000). According to WoLF PSORT (Horton *et al*., 2007) ERF103 has a single nuclear localisation signal (NLS) whereas ERF102, ERF104 and ERF105 have two NLS (Figure 1a).

Comparison of the amino acid sequences of ERF102 to ERF105 using MUSCLE (Edgar, 2004) revealed a sequence identity of 40 % between all four proteins with high conservation of the AP2/ERF domain. The protein pairs share 67 % (ERF102 and ERF103) and 52 % (ERF104

bioRxiv preprint doi: https://doi.org/10.1101/848705; this version posted November 20, 2019. The copyright holder for this preprint (which was not certified by peer review) is the author/funder, who has granted bioRxiv a license to display the preprint in perpetuity. It is made available under aCC-BY-NC-ND 4.0 International license.

and ERF105) amino acid identity. Phylogenetic analysis confirmed that ERF102 to ERF105 are closely related, with ERF102 and ERF103 together on one branch and ERF104 and ERF105 on the other branch of the phylogenetic tree (Figure 1b).

The *ERF102* to *ERF105* transcription factor genes show a similar transcriptional regulation pattern

Analysis of transcriptional regulation may yield indications on functional context, therefore the previous work showing that *ERF102* to *ERF105* are regulated similarly by cold and different cold stress-related hormones, including ethylene, jasmonate and abscisic acid (Bolt *et al*., 2017), was extended. First we complemented the comparison of the hormonal transcriptional regulation of the four *ERF* genes and analysed their response to auxin and salicylic acid (SA). Auxin (NAA) rapidly and strongly induced the transcript abundances of all four *ERF* genes about 180-fold (*ERF102*), 100-fold (*ERF103*), 13-fold (*ERF104*) and 130-fold (*ERF105*) after 30 min. This increase was transient as 2 h after auxin treatment the transcript abundances were only increased between 11-fold (*ERF102*) and 2-fold (*ERF105*) (Figure 2a). In contrast, the transcript levels of all four *ERF* genes were downregulated by SA to about 50 % of the initial level after 2 h (Figure 2b).

Next, the response to different stress treatments was studied. Heat stress (42 °C) induced an upregulation of *ERF104* and *ERF105* of about 5-fold and 8-fold, respectively, after 2 h (Figure 2c). High light (1000 µmol m^{-2} s^{-1}) provoked a rapid upregulation of all four genes about 4-fold (*ERF102*), 3-fold (*ERF103* and *ERF104*) and 4.5-fold (*ERF105*) after 30 min. The transcripts were back to their initial levels after 2 h (Figure 2d). Oxidative stress imposed by H_2O_2 treatment resulted in a rapid upregulation of all four genes after 15 min by about 3.5-fold (*ERF102*), 4.5-fold (*ERF103*), 6.5-fold (*ERF104*), and 8.5-fold (*ERF105*). After 2 h transcript levels were increased further to about 5-fold (*ERF102*), 9-fold (*ERF103*), 10-fold (*ERF104*) and 12-fold (*ERF105*) compared to the initial level (Figure 2e). Oxidative stress imposed by

bioRxiv preprint doi: https://doi.org/10.1101/848705; this version posted November 20, 2019. The copyright holder for this preprint (which was not certified by peer review) is the author/funder, who has granted bioRxiv a license to display the preprint in perpetuity. It is made available under aCC-BY-NC-ND 4.0 International license.

281 treatment with the superoxide-generating herbicide paraquat showed a similar result (Figure 2f).
282 A fast transcriptional response of the *ERF* genes was also observed after drought stress that led
283 to an about 2-fold (*ERF102* and *ERF104*), 3.5-fold (*ERF103*) and 5.5-fold (*ERF105*)
284 upregulation of transcript levels within 15 min, which were decreased again after 1 h
285 (Figure 2g). Salt stress (200 mM NaCl) also caused a rapid but transient upregulation of the
286 *ERF* genes up to about 6–7-fold for the *ERF102*, *ERF103* and *ERF105* genes (Figure 2h). Two
287 of the genes (*ERF102*, *ERF105*) also responded rapidly to mannitol application (Figure 2i).
288 Taken together, the four *ERF* genes showed similar, very rapid and often transient
289 transcriptional responses to different plant hormones, including an extraordinarily strong
290 induction by auxin, as well as rapid, strong and often comparable responses to different stress
291 treatments. Some individual response profiles such as stronger responses to heat by *ERF104*
292 and *ERF105* or the lack of response to NaCl and mannitol by *ERF104* were observed as well.
293 These partly similar stress response profiles would be consistent with overlapping functions in
294 response to these stresses.

295

296 ***pERF102:GUS* to *pERF105:GUS* reporter genes are expressed in different tissues in**
297 ***Arabidopsis thaliana***

298 Transgenic plants expressing the *GUS* reporter gene under the control of ~2 kb of the
299 *ERF102* to *ERF104* promoters located 5´ upstream of the coding regions were analysed to
300 determine the tissue-specific expression of these genes.
301 Thirty h after imbibition, strong GUS activity of *pERF102:GUS* plants was detected in the
302 root tip transition zone of germinated seedlings (Figure 3a) and expanded within the next 30 h
303 within the radicle (Figure 3b). Ten DAG, *pERF102:GUS* was expressed in all root tissues except
304 root tips and root hairs. The strongest GUS activity was observed in the vascular bundle of
305 primary roots and in cortex cells that surround emerging lateral roots (Figure 3c–e). Weak

bioRxiv preprint doi: https://doi.org/10.1101/848705; this version posted November 20, 2019. The copyright holder for this preprint (which was not certified by peer review) is the author/funder, who has granted bioRxiv a license to display the preprint in perpetuity. It is made available under aCC-BY-NC-ND 4.0 International license.

306 *pERF102:GUS* expression was detected in the shoot apical meristem (SAM) of seedlings
307 (Figure 3f).

308 *pERF103:GUS* activity was detected 60 h after imbibition in the root tip (Figure 3g) and
309 seven DAG in the whole root (Figure 3h). Very high activity was detected in the root apical
310 meristem (RAM) (Figure 3j). *pERF103:GUS* was also expressed in the root tip of lateral roots,
311 but only after stage VIII of lateral root development (Péret *et al*., 2009) (Figure 3k). GUS activity
312 was observed in the vasculature of primary roots (Figure 3l), but not in the vasculature of
313 emerging or fully developed lateral roots, and in cortex cells that surround emerging lateral roots
314 (Figure 3m). In shoot tissues, weak expression of *pERF103:GUS* was detected only in the shoot
315 apex (Figure 3i).

316 *pERF104:GUS* expression was also detected early after germination. Sixty h after
317 imbibition, *pERF104:GUS* was weakly expressed in the vasculature of hypocotyls and
318 cotyledons and slightly stronger in the vasculature of radicles (Figure 3n). Seven-day-old
319 seedlings showed GUS activity in the vascular tissues as well as in the shoot apex (Figure 3o–
320 q). A particularly well-defined local GUS signal was noted in the quiescent center of roots
321 (Figure 3r and 3s). In addition, GUS activity was detected in the style of the gynoecium and at
322 the base and in the apex of siliques (Figure 3t and 3u).

323 As plants matured, GUS activity of *pERF102:GUS* to *pERF104:GUS* plants was present in
324 the same tissues as in young seedlings but declined progressively (data not shown). Together,
325 *promoter:GUS* fusions of all three *ERF* genes were predominantly expressed in root tissues,
326 similar to *pERF105:GUS* (Bolt *et al*., 2017).

327

328 **GFP-ERF102 to GFP-ERF105 are located in the nucleus**

329 To examine the subcellular localisation of the ERF102 to ERF104 proteins, full-length
330 cDNAs of *ERF102* to *ERF104* were fused in frame to the 3' end of the *GREEN FLUORESCENT*
331 *PROTEIN* (*GFP*) coding sequence. The resulting *GFP-ERF102*, *GFP-ERF103* and

bioRxiv preprint doi: https://doi.org/10.1101/848705; this version posted November 20, 2019. The copyright holder for this preprint (which was not certified by peer review) is the author/funder, who has granted bioRxiv a license to display the preprint in perpetuity. It is made available under aCC-BY-NC-ND 4.0 International license.

GFP-ERF104 fusion genes driven by the cauliflower mosaic virus (CaMV) *35S* promoter were transiently expressed in *Nicotiana benthamiana* leaf cells. Confocal imaging of GFP fluorescence in leaf cells showed that all three fusion proteins were predominantly located in the nucleus, weaker signals were derived from the cytosol (Figure 4). This pattern was similar to the predominant nuclear localisation of GFP-ERF105 (Bolt *et al*., 2017).

Characterisation of plants with altered *ERF102* to *ERF105* expression levels

To identify and compare biological functions of the *ERF102* to *ERF104* genes, we studied transgenic lines with altered expression levels. For *ERF102*, a homozygous T-DNA insertion line (*erf102*; SAIL_46_C02) was obtained. Verification of the annotated location of the T-DNA insertion in *erf102* by sequencing revealed that the T-DNA is located at position +507 within the AP2/ERF domain (Figure S1a). RT-PCR analysis did not detect any expression of *ERF102* in *erf102* plants, suggesting that it is a null allele (Figure S1b). The morphological phenotype of the *erf102* mutant described below (Figure S2e) was fully complemented by introgression of the *35S:ERF102* gene (Figure S1c–1f). In several available T-DNA insertion lines for *ERF103* (SALK_087356, GABI_085B06) or *ERF104* (SALK_024275, SALK_057720, SALK_152806) we detected residual *ERF* expression. Therefore, lines with a reduced *ERF103* or *ERF104* expression were constructed using artificial microRNAs (amiRNAs) (Schwab *et al*. 2006). Two independent, homozygous amiRNA expressing lines with the lowest residual expression of the target genes were selected for further experiments (Figure S2a and Bolt *et al*., 2017). Moreover, lines overexpressing *ERF102* to *ERF104* under control of the CaMV *35S* promoter were constructed and two strongly expressing lines selected (Figure S2b–2d).

Morphological analysis of plants with reduced or increased *ERF102* to *ERF104* expression revealed in most cases only slight differences of shoot growth compared to wild-type plants. Furthermore, plants with altered expression of *ERF102*, *ERF103* or *ERF104* flowered at

bioRxiv preprint doi: https://doi.org/10.1101/848705; this version posted November 20, 2019. The copyright holder for this preprint (which was not certified by peer review) is the author/funder, who has granted bioRxiv a license to display the preprint in perpetuity. It is made available under aCC-BY-NC-ND 4.0 International license.

the same time as wild-type plants and showed a similar onset of leaf senescence (data not shown). In contrast, root elongation, the formation of lateral roots as well as the lateral root density was more strongly affected by altered expression of these genes (Figure 5c–5e).

The *erf102* mutant exhibited an about 10 % reduced shoot height compared to the wild type. Overexpressing lines of *ERF102* exhibited a slightly but not significantly increased shoot height as well as a 10 % (ERF102ox-1) and 8 % (ERF102ox-2) bigger rosette diameter (Figure 5a and 5b). Moreover, ten DAG *erf102* exhibited 27 % less and ERF102ox-1 and ERF102ox-2 48 % and 51 % more lateral roots compared to wild type (Figure 5d). Lateral root density was increased 29–31 % in the ERF102ox lines (Figure 5e).

Both 35S:ami103 lines were smaller in size, with an 8 % reduced shoot height and a 6–9 % reduced rosette diameter compared to the wild type, while *ERF103* overexpression did not cause phenotypic differences in shoot height and rosette size (Figure 5a and 5b). Primary root elongation was about 13 % lower in both 35S:ami103 lines whereas ERF103ox-1 and ERF103ox-2 exhibited 12 % and 17 % longer primary roots compared to wild type (Figure 5c). Similarly, 35S:ami103 lines had up to 32 % less and ERF103ox plants up to 31 % more lateral roots than wild type (Figure 5d).

35S:ami104 lines had a 9 % (35S:ami104-1) and 18 % (35S:ami104-2) reduced shoot height, but an unchanged rosette diameter (Figure 5a and 5b). Primary root elongation of 35S:ami104 lines was slightly reduced (about 13 % in 35S:ami104-2) and enhanced by up to 29 % in *ERF104* overexpressing lines (Figure 5c). The number of lateral roots was reduced by about 20 % in both 35S:ami104 lines, while ERF104ox-1 and ERF104ox-2 exhibited 57 % and 53 % more lateral roots (Figure 5d) and had a 30 % and 22 % higher lateral root density compared to wild type (Figure 5e).

Bolt *et al*. (2017) described that the shoot phenotype of *erf105* and ERF105ox lines resembled the wild type. Here, root analysis revealed 23 % less lateral roots in the *erf105* mutant compared to wild type (Figure 5c). ERF105ox lines showed a 17-25 % higher primary

bioRxiv preprint doi: https://doi.org/10.1101/848705; this version posted November 20, 2019. The copyright holder for this preprint (which was not certified by peer review) is the author/funder, who has granted bioRxiv a license to display the preprint in perpetuity. It is made available under aCC-BY-NC-ND 4.0 International license.

root elongation, 53-83 % more lateral roots and a 31-44 % higher lateral root density compared to wild type (Figure 5c–5e).

To examine a potentially redundant role of the four *ERF* genes, several higher order mutants were generated, namely *erf102* 35S:amiERF103, *erf102* 35S:amiERF104, *erf105* 35S:amiERF103, and *erf102* 35S:amiERF104/105. These lines include all possible combinations of at least two *ERF* genes that are mutated or have a lowered expression, except combined loss of function of *ERF103* and *ERF104*. Higher order mutants did not show a phenotypic additive effect compared to the respective single mutants with respect to rosette diameter, shoot height, primary root elongation, number of lateral roots and flowering time (data not shown). These results suggest that *ERF102* to *ERF105* are not acting redundantly on growth regulation. However, we cannot exclude that the degree of downregulation achieved by amiRNAs is insufficient to uncover redundant gene activities.

Analysis of the functional redundancy of the *ERF102* to *ERF105* genes in the cold acclimation response

ERF105 is a positive regulator of *Arabidopsis* freezing tolerance and cold acclimation (Bolt *et al*., 2017). Therefore, we analysed whether the *ERF102* to *ERF104* genes, which are also regulated by cold (Bolt *et al*., 2017; Lee *et al*., 2005; Park *et al*., 2015; Vogel *et al*., 2005), also play a role in regulating freezing tolerance and cold acclimation. To this end, we studied the transcript accumulation of selected cold responsive genes in *ERF* single and double mutants and analysed the freezing tolerance of these mutants.

First, we examined the expression levels of selected cold-responsive genes in plants with reduced or enhanced expression of a single *ERF102* to *ERF104* gene before (non-acclimated, NA) and after 14 d of cold acclimation (ACC14) and compared these to wild type. The transcript levels of cold-responsive genes were in all lines similar to wild type (Figure

bioRxiv preprint doi: https://doi.org/10.1101/848705; this version posted November 20, 2019. The copyright holder for this preprint (which was not certified by peer review) is the author/funder, who has granted bioRxiv a license to display the preprint in perpetuity. It is made available under aCC-BY-NC-ND 4.0 International license.

S3), which contrasts with the strongly altered transcript levels displayed by the *erf105* mutant and *ERF105* overexpressing lines (Bolt *et al.*, 2017).

The analysis of higher order mutants revealed that under non-acclimated (NA) conditions the steady state mRNA levels of *CBF1*, *CBF2*, *COR15A*, and *COR15B* were up to 60 % lower in the *erf105* 35S:ami103-1 plants compared to those of the wild type (Figure 6). In all other mutant combinations the basic expression level of these cold-responsive genes was slightly, but not significantly lower than in the wild type. After 14 d of acclimation at 4 °C (ACC14), the expression levels of these genes were elevated between 2- and 5-fold in wild type compared to NA plants. ACC14 plants with mutated *ERF102* or *ERF105* genes combined with reduced expression of *ERF103* or *ERF104* showed, in most cases, a lower induction of the cold-responsive genes. For example, the induction levels of *CBF2* and *COR15B* were reduced in all hybrid lines to about 50 % of the wild-type level. Strikingly, the induction of *CFB3* was completely absent in all mutant lines while it was induced about 2-fold in wild type. In contrast, *ZAT12* gene expression showed a stronger increase in *erf102* 35S:ami103-1, *erf102* 35S:ami104-2 and *erf105* 35S:ami103-1 than in wild type (Figure 6f).

Next, we determined the freezing tolerance of plants with reduced *ERF102, ERF103* and *ERF104* gene expression before and after 14 d of cold acclimation at 4 °C by an electrolyte leakage assay of detached leaves (Thalhammer *et al*., 2014). To take into account the almost complete arrest of plant growth at 4 °C, the electrolyte leakage assay was performed at the same developmental state for both NA and ACC plants. *erf105* mutant plants used as positive control showed higher LT_{50} (temperature of 50 % electrolyte leakage) values (-3.99 ± 0.13 °C in NA plants and -8.99 ± 0.17 °C in ACC14 plants) compared to wild type (-4.7 ± 0.11 °C in NA plants and -10.82 ± 0.12 °C in ACC14 plants) (Figure 7a), which is consistent with previous results (Bolt *et al*., 2017). In contrast, *erf102*, 35S:ami103-1 and 35S:ami104-2 plants did not show differences in LT_{50} values compared to wild type. Also, overexpression of single *ERF102*,

bioRxiv preprint doi: https://doi.org/10.1101/848705; this version posted November 20, 2019. The copyright holder for this preprint (which was not certified by peer review) is the author/funder, who has granted bioRxiv a license to display the preprint in perpetuity. It is made available under aCC-BY-NC-ND 4.0 International license.

433 *ERF103* or *ERF104* genes did not lead to altered freezing tolerance under NA conditions
434 (Figure S4). The behavior of the overexpressing lines in response to acclimation was not tested.
435 Analysis of the freezing tolerance of higher order mutants revealed that only the *erf105*
436 35S:ami103-1 plants showed higher LT_{50} values (-4.93 ± 0.12 °C) compared to wild type
437 (-5.46 ± 0.12 °C) under NA conditions (Figure 7b). Following cold acclimation, several
438 combinations exhibited higher LT_{50} values compared to wild type (-9.54 ± 0.18 °C). The
439 strongest change was shown by *erf102* 35S:ami103-1 (-7.89 ± 0.24 °C), while
440 *erf105* 35S:ami103-1 (-8.78 ± 0.25 °C) as well as *erf102* 35S:ami104/105-1 (-8.79 ± 0.25 °C)
441 showed smaller effects. In contrast, *erf102* 35S:ami104-2 showed a similar LT_{50} as wild type
442 after cold acclimation (Figure 7b).
443
444 **DISCUSSION**
445 Recently, we reported that *ERF102* to *ERF105* are regulated by cold and different cold stress-
446 related hormones, and we demonstrated that *ERF105* has a function in the freezing tolerance
447 and cold acclimation of *Arabidopsis* (Bolt *et al*., 2017). In the present study we significantly
448 extended this work and first investigated further expression characteristics of the gene family
449 members and then explored their potentially redundant roles in regulating plant growth and the
450 cold acclimation response.
451
452 *The* ERF102 *to* ERF105 *genes show overlapping expression patterns*
453 The similar profiles of gene expression in response to hormone or stress treatment are
454 consistent with a partial functional redundancy of *ERF102* to *ERF105*. For instance, all genes
455 were rapidly downregulated by SA (Figure 2b) and upregulated by high light or H_2O_2 (Figure 2e
456 and 2f). Network analysis of publicly available transcriptome data using for instance
457 GeneMANIA (Warde-Farley *et al*., 2010) also showed that these four *ERF* genes are co-
458 regulated and co-expressed in a large number of conditions including numerous hormone and

bioRxiv preprint doi: https://doi.org/10.1101/848705; this version posted November 20, 2019. The copyright holder for this preprint (which was not certified by peer review) is the author/funder, who has granted bioRxiv a license to display the preprint in perpetuity. It is made available under aCC-BY-NC-ND 4.0 International license.

chemical treatments (Figure S5). However, some individual response profiles were discovered as well. Thus, not all four *ERF* genes were transcriptionally regulated by heat, drought, NaCl, or mannitol (Figure 2). Together, the analysis of transcriptional regulation is in line with the idea that *ERF102* to *ERF105* have roles in multiple hormone and stress responses as was shown for these and other ERFs in a number of cases (Bethke *et al.*, 2009; Dubois *et al*., 2013, 2015; reviewed by Licausi, Ohme-Takagi & Perata 2013; Mase *et al*., 2013; Meng *et al*., 2013; Moffat *et al*., 2012; Moore *et al*., 2014; Sewelam *et al*., 2013; Son *et al*., 2012; Vogel *et al*., 2014; Xie *et al.*, 2019).

The ERF102 *to* ERF105 *genes have a limited impact on plant growth*

The tissue-specific expression patterns of *pERF102:GUS* to *pERF105:GUS* are partly overlapping, which is in accordance with a redundant function of the ERF proteins. All four genes are predominantly expressed in the root, only for *pERF105:GUS* a significant expression was detected also in several shoot tissues such as vasculature, apical shoot and stomata (Bolt *et al.*, 2017). Expression of all four *pERF-GUS* reporter genes was visible shortly after germination in different cell types of the radicle and later in distinct root tissues and cell types. For example, *pERF102:GUS*, *pERF103:GUS* and *pERF105:GUS* were expressed in the cortex cells that surround emerging lateral roots. Interestingly, expression of *ERF102*, *ERF103* and *ERF105* is regulated by cytokinin and auxin, two key hormones of lateral root development (Benková *et al*., 2003; Casimiro *et al*., 2003; Chang, Ramireddy & Schmülling, 2013, 2015; Swarup *et al*., 2008). However, insertional mutants or amiRNA lines did not reveal a major role of these genes in regulating root architecture. 35S:ami103 and 35S:ami104 lines had shorter roots and most loss-of-function mutants formed less lateral roots. However, the differences were small and the lateral root density mostly not significantly altered (Figure 5c-e). Opposite and stronger phenotypic changes were noted in the respective overexpressing lines, which had longer roots, an increased number (by up to ~85 %) of lateral roots and a higher lateral root

bioRxiv preprint doi: https://doi.org/10.1101/848705; this version posted November 20, 2019. The copyright holder for this preprint (which was not certified by peer review) is the author/funder, who has granted bioRxiv a license to display the preprint in perpetuity. It is made available under aCC-BY-NC-ND 4.0 International license.

density. Although overexpression experiments may produce artefacts and are not fully conclusive they have been often informative about the functional context of a given gene. Loss-of-function phenotypes of genes regulating root architecture can be subtle or depend on the environmental or developmental context (Motte, Vanneste & Beeckman, 2019) and thus might have gone unnoticed in the *erf* mutants. The strong regulation of the four *ERF* genes by different stressors suggests that they might be particularly relevant under stressful conditions. It cannot be excluded that members of the *ERF105* gene subfamily studied here contribute to regulating root architecture under specific environmental conditions, this requires further investigation.

Among the expression sites of the four *ERF* genes, the expression of *pERF104:GUS* in the quiescent center (Figure 3r) particularly intriguing. Noteworthy, among the direct targets of ERF104 is the transcription factor gene *SCARECROW* (*SCR*) (Sparks *et al*., 2016). SCR is, together with SHORTROOT, essential for quiescent center specification and maintenance (Salvi *et al*., 2018; reviewed by Benfey, 2016). Further, in a yeast two-hybrid screen the transcription factor MYB56/BRASSINOSTEROIDS AT VASCULAR AND ORGANIZING CENTER (BRAVO) was identified as an interactor of ERF104 (our unpublished result). MYB56/BRAVO represses cell divisions in the quiescent center thus counteracting SCR (Di Laurenzio *et al*., 1996; Vilarrasa-Blasi *et al*., 2014). It is known that interaction with other transcription factors modulates the activity of ERFs (Licausi *et al*., 2013; Xie *et al*., 2019). While these data suggest that ERF104 might be part of the transcription factor network in the quiescent center, we have been unable to detect any changes of cellular organisation in the quiescent center and surrounding cells nor did we detect altered *SCR* gene expression in the 35S:ami104 and ERF104ox lines (data not shown). It could be that the decrease in *ERF104* expression obtained in the amiRNA lines is not sufficient to cause a strong loss-of-function phenotype, analysis of a null mutation could be more informative.

bioRxiv preprint doi: https://doi.org/10.1101/848705; this version posted November 20, 2019. The copyright holder for this preprint (which was not certified by peer review) is the author/funder, who has granted bioRxiv a license to display the preprint in perpetuity. It is made available under aCC-BY-NC-ND 4.0 International license.

511 *The* ERF102 *to* ERF105 *genes redundantly regulate the response to cold stress*

512 One important goal of this work was to analyse the possible roles of the ERF105-related
513 transcription factors in the response to cold stress. *ERF102* to *ERF105* are rapidly cold-induced
514 (Bolt *et al*., 2017) in parallel with the first wave transcription factors of the cold stress response
515 including the *CBF* genes (Park *et al*., 2015). Mutation or reduced expression of *ERF102,*
516 *ERF103* or *ERF104* single genes did not lead to an altered freezing tolerance. In case of the
517 amiRNA lines this could be due to residual gene expression (Figure 7a and S1). Thus, among
518 the four genes only the mutation of *ERF105* resulted in a decreased freezing tolerance before
519 and after cold acclimation compared to wild type underpinning its primary role (Figure 7a and
520 Bolt *et al.*, 2017). However, the analysis of freezing tolerance of higher order mutants indicated
521 that *ERF102* and *ERF103* also play a role in cold acclimation, since the reduced expression of
522 both genes resulted in altered expression of cold response genes (Figure 6) and higher freezing
523 sensitivity (Figure 7b). The eventual role of ERF104 cannot be determined with certainty as only
524 amiRNA lines were available and not all combinations with other *ERF* genes were tested.
525 35S:ami104 lines in combination with the *erf102* mutation showed an altered expression of cold-
526 responsive genes similar to other double mutant combinations (Figure 6) and the LT_{50} value
527 was higher than in wild type although the significance was below the threshold ($p < 0.05$),
528 indicating that ERF104 might be involved in the response to cold as well. Our attempts to
529 demonstrate a role of these *ERF* genes at low temperatures in the root as was reported for
530 *CRF2* and *CRF3* belonging to a different class of *ERF* genes (Jeon et al., 2016), have failed.
531 Such an activity could, as was stated above, be masked by incomplete loss of function and/or
532 the unknown nature of their specific activities.

533 Based on transcript data which show a lowered activation of *CBF* and *COR* genes in *erf*
534 gene mutants after cold acclimation (Figure 6), ERF102, ERF103 and ERF104 may also play a
535 role upstream of these genes as was suggested for ERF105 (Bolt *et al*., 2017). Increased *CBF3*
536 expression upon cold acclimation was even completely lacking in the *erf* mutants (Figure 6c) but

bioRxiv preprint doi: https://doi.org/10.1101/848705; this version posted November 20, 2019. The copyright holder for this preprint (which was not certified by peer review) is the author/funder, who has granted bioRxiv a license to display the preprint in perpetuity. It is made available under aCC-BY-NC-ND 4.0 International license.

537 the gene was still cold responsive at earlier time points although with a reduced amplitude as
538 compared to wild type (Figure S6). A proximity of the four *ERF* genes to the CBF regulon was
539 also suggested by the result of the network analysis which placed several proteins that are part
540 of the CBF regulon (CBF2/DREB1c, ZAT10 und RAP2.13/RAP2.4) in the vicinity of ERF102 to
541 ERF105 (Figure S5).

542 The lower activation of the *CBF* and *COR* genes in cold-acclimated *erf* gene mutants could
543 be at least partially due to enhanced expression of another gene belonging to the CBF regulon,
544 *ZAT12* (Figure 6f). *ZAT12* encodes a zinc-finger protein known to be a negative regulator of the
545 CBF regulon and is usually induced in parallel with *CBF* and *COR* genes providing a negative
546 regulatory feedback loop (Vogel *et al*., 2005). The higher expression of *ZAT12* in the *erf* higher
547 order mutants suggests that these *ERF* genes may act as negative regulators of *ZAT12*
548 expression and in this way as positive regulators of *CBF* and *COR* genes. Notably, the *ZAT12*
549 gene does not possess the specific DNA-binding motif of ERF transcription factors, the GCC-
550 box, in its promoter region (Hao *et al*., 1998) suggesting that additional factors might be required
551 for its repression by ERFs.

552 Knockout/knockdown of single *ERF102* to *ERF104* genes did not cause an altered
553 transcript level of cold-responsive genes after 14 d of cold acclimation (Figure S3), which is
554 again in line with the assumption that these *ERF* genes may have redundant roles. Lines
555 overexpressing *ERF102* to *ERF104* did neither show a differential expression of cold-
556 responsive genes nor an altered freezing tolerance (Figure S3 and S4), similar to *ERF105*
557 overexpressing lines (Bolt *et al*., 2017). It is possible that ERF102 to ERF105 are required for
558 the transcriptional activation of these target genes but are not the rate-limiting factors, for
559 example because they function as part of a complex. Alternatively, activity of these proteins
560 under cold may depend on additional regulatory steps such as phosphorylation which could be
561 transient. Indeed, the phosphorylation of ERF102 to ERF104 by MPK3 and/or MPK6 was shown
562 (Bethke *et al*., 2009; Son *et al*., 2012; Wang, Du, Zhao, Miao & Song, 2013) and functions of

bioRxiv preprint doi: https://doi.org/10.1101/848705; this version posted November 20, 2019. The copyright holder for this preprint (which was not certified by peer review) is the author/funder, who has granted bioRxiv a license to display the preprint in perpetuity. It is made available under aCC-BY-NC-ND 4.0 International license.

563 MPK3 and MPK6 in the cold signalling pathway have been described (Kim *et al*., 2017; Li *et al*.,
564 2017; Zhao *et al*., 2017).

565 Taken together, the data document redundant functions of *ERF102* to *ERF105* in response
566 to cold. Notably, combined action of related *ERF* transcription factor genes has also been
567 reported in other cases (Jeon, Cho, Lee, Van Binh & Kim, 2016; Kim, Jang & Park, 2016).
568 Future work will investigate how the ERF102 to ERF105 proteins are integrated in the extensive
569 transcriptional network governing the response to cold.

570

571 **SUPPORTING INFORMATION**

572 **Figure S1. Characterisation of the *erf102* mutant SAIL_46_C02.** (a) Structure of the
573 *Arabidopsis ERF102* (AT5G47230) gene. The black line denotes the untranslated region, the
574 black box represents the exon, the T-DNA insertion at position +507 is shown by a triangle. The
575 positions of primers that were used for RT-PCR are indicated by arrows. (b) RT-PCR analysis of
576 *ERF102* expression using total RNA extracted from seedlings of wild type and *erf102*. The
577 *Actin2* gene was used as internal control. (c–f) Complementation of the *erf102* mutant by
578 introgression of the *35S:ERF102* gene. Shoot height (c) and rosette diameter (d) of 35-day-old
579 plants. (e) Elongation of the primary root and (f) number of lateral roots of plants grown on half-
580 strength MS medium. Asterisks indicate significant differences to the wild type ($n \geq 30$),
581 (*, $p < 0.05$; **, $p < 0.01$). Error bars represent SE.

582

583 **Figure S2. Analysis of lines with altered *ERF102* to *ERF104* expression levels.** (a–d)
584 Relative expression level of *ERF* genes in eight pooled eleven-day-old seedlings of wild type,
585 lines expressing amiRNA directed against *ERF103* (a) and lines overexpressing *ERF102* (b),
586 *ERF103* (c,) or *ERF104* (d). Transcript levels of wild-type samples were set to 1 ($n \geq 4$).
587 Asterisks indicate significant differences to the wild type (***, $p < 0.001$). Error bars represent

bioRxiv preprint doi: https://doi.org/10.1101/848705; this version posted November 20, 2019. The copyright holder for this preprint (which was not certified by peer review) is the author/funder, who has granted bioRxiv a license to display the preprint in perpetuity. It is made available under aCC-BY-NC-ND 4.0 International license.

588 SE. (e–g) Shoot phenotype of plants grown 35 days under long day conditions. The pictures are
589 complementary to the data shown in Figure 5a and 5b.
590
591 **Figure S3. Expression of selected cold-responsive genes in lines with reduced or**
592 **enhanced *ERF102* to *ERF104* expression.** Relative expression of *CBF1* (a), *CBF2* (b),
593 *COR15A* (c), and *COR15B* (d) genes in lines with reduced or enhanced *ERF102* to *ERF104*
594 expression before (non-acclimated, NA) and after 14 days (acclimated, ACC14) of cold
595 acclimation at 4 °C. Transcript levels of wild-type samples under non-acclimated conditions
596 were set to 1 ($n \geq 4$). Error bars represent SE.
597
598 **Figure S4. Electrolyte leakage assays of lines with enhanced *ERF102* to *ERF104***
599 **expression.** Electrolyte leakage assays on detached leaves of lines overexpressing *ERF102*,
600 *ERF103* or *ERF104* before (non-acclimated, NA) and after 14 days (acclimated, ACC14) of cold
601 acclimation at 4 °C. The bars represent the means ± SE from four replicate measurements
602 where each replicate comprised leaves from three plants.
603
604 **Figure S5. Network of co-localisation, co-expression, genetic and physical interactions of**
605 **ERF105.** The blue connecting lines between two genes represent co-localisation, purple lines
606 co-expression, green lines genetic interactions and red lines physical interactions. ABI1, ABA
607 INSENSITIVE 1; AZF3, ZINC-FINGER PROTEIN 3; CAF1-9, CCR4-ASSOCIATED FACTOR 1
608 HOMOLOG 9; CYP707A3, CYTOCHROME P450, FAMILY 707, SUBFAMILY A,
609 POLYPEPTIDE 3; DREB1C (CBF2), DEHYDRATION-RESPONSE ELEMENT-BINDING
610 PROTEIN 1C/C-REPEAT-BINDING FACTOR 2; ERF, ETHYLENE RESPONSE FACTOR;
611 PP2CA, PROTEIN PHOSPHATASE 2CA; PUMP4, PLANT UNCOUPLING MITOCHONDRIAL
612 PROTEIN 4; RAP2-13 (RAP2.4/WIND), RELATED TO AP2 13; SZF1, SALT-INDUCIBLE ZINC-

bioRxiv preprint doi: https://doi.org/10.1101/848705; this version posted November 20, 2019. The copyright holder for this preprint (which was not certified by peer review) is the author/funder, who has granted bioRxiv a license to display the preprint in perpetuity. It is made available under aCC-BY-NC-ND 4.0 International license.

613 FINGER; ZAT10 (STZ), ZINC FINGER PROTEIN 10 (SALT TOLERANCE ZINC FINGER).
614 Analysis was done using GeneMANIA (Warde-Farley *et al*., 2010).
615
616 **Figure S6. Expression of selected cold-responsive genes in lines with reduced *ERF102* to**
617 ***ERF105* expression.** Relative expression of *CBF1*, *CBF2* and *CFB3* genes in lines with
618 reduced *ERF102* to *ERF105* after 4 h of cold treatment at 4 °C. Transcript levels of wild-type
619 samples under control conditions were set to 1 ($n \geq 4$). Asterisks indicate significant differences
620 to the wild type (*, $p < 0.05$; ***, $p < 0.001$). Error bars represent ± SE.
621
622 **Table S1. Sequences of primers used for cloning.** Small letters in the primer sequences
623 indicate the integrated *attB4*- or *attB1*-sites for cloning DNA fragments into the vector pDONR
624 P4-P1R. Small italic letters in the primer sequences indicate the integrated *attB1*- or *attB2*-sites
625 for cloning DNA fragments into the vector pDONR221. Underlined letters are the nucleotides
626 added to keep the sequence in the right frame.
627
628 **ACKNOWLEDGEMENTS**
629 We acknowledge funding by Deutsche Forschungsgemeinschaft (Collaborative Research
630 Centre 973, www.sfb.973).
631
632 **REFERENCES**
633 Abràmoff M.D., Magalhaes P.J. & Ram S.J. (2004) Image processing with ImageJ. *Journal of*
634 *Biophotonics* 11, 36–43.
635 Agarwal M., Hao Y., Kapoor A., Dong C.H., Fujii H., Zheng X. & Zhu J.K. (2006a) A R2R3 type
636 MYB transcription factor is involved in the cold regulation of *CBF* genes and in acquired
637 freezing tolerance. *Journal of Biological Chemistry* 281, 37636–37645.

bioRxiv preprint doi: https://doi.org/10.1101/848705; this version posted November 20, 2019. The copyright holder for this preprint (which was not certified by peer review) is the author/funder, who has granted bioRxiv a license to display the preprint in perpetuity. It is made available under aCC-BY-NC-ND 4.0 International license.

638 Agarwal P.K., Agarwal P., Reddy M.K. & Sopory S.K. (2006b) Role of DREB transcription
639 factors in abiotic and biotic stress tolerance in plants. *Plant Cell Reports* 25, 1263–1274.
640 Benfey PN (2016). Defining the path from stem cells to differentiated tissue. *Current Topics*
641 *Developmental Biology* 116, 35–43.
642 Benková E., Michniewicz M., Sauer M., Teichmann T., Seifertová D., Jürgens G. & Friml J.
643 (2003) Local, efflux-dependent auxin gradients as a common module for plant organ
644 formation. *Cell* 115, 591–602.
645 Bethke G., Unthan T., Uhrig J.F., Pöschl Y., Gust A.A., Scheel D. & Lee J. (2009) Flg22
646 regulates the release of an ethylene response factor substrate from MAP kinase 6 in
647 *Arabidopsis thaliana* via ethylene signaling. *Proceedings of the National Academy of*
648 *Sciences USA* 106, 8067–8072.
649 Bolt S., Zuther E., Zintl S., Hincha D.K. & Schmülling T. (2017) ERF105 is a transcription factor
650 gene of *Arabidopsis thaliana* required for freezing tolerance and cold acclimation. *Plant Cell*
651 *Environment* 40, 108–120.
652 Brenner W.G., Romanov G.A., Köllmer I., Bürkle L. & Schmülling T. (2005) Immediate-early and
653 delayed cytokinin response genes of *Arabidopsis thaliana* identified by genome-wide
654 expression profiling reveal novel cytokinin-sensitive processes and suggest cytokinin action
655 through transcriptional cascades. *The Plant Journal* 44, 314–333.
656 Cao F.Y., Khan M., Taniguchi M., Mirmiran A., Moeder W., Lumba S., Yoshioka K. & Desveaux
657 D. (2019) A host-pathogen interactome uncovers phytopathogenic strategies to manipulate
658 plant ABA responses. *The Plant Journal*, doi: 10.1111/tpj.14425.
659 Casimiro I., Beeckman T., Graham N., Bhalerao R., Zhang H., Casero P., … & Bennett M.J.
660 (2003) Dissecting *Arabidopsis* lateral root development. *Trends in Plant Science* 8, 165–
661 171.

bioRxiv preprint doi: https://doi.org/10.1101/848705; this version posted November 20, 2019. The copyright holder for this preprint (which was not certified by peer review) is the author/funder, who has granted bioRxiv a license to display the preprint in perpetuity. It is made available under aCC-BY-NC-ND 4.0 International license.

662 Chang L., Ramireddy E. & Schmülling T. (2013) Lateral root formation and growth of
663 Arabidopsis is redundantly regulated by cytokinin metabolism and signalling genes. *Journal*
664 *of Experimental Botany* 64, 5021–5032.
665 Chang L., Ramireddy E. & Schmülling T. (2015) Cytokinin as a positional cue regulating lateral
666 root spacing in Arabidopsis. *Journal of Experimental Botany* 66, 4759–4768.
667 Chinnusamy V., Ohta M., Kanrar S., Lee B.H., Hong X., Agarwal M. & Zhu J.K. (2003) ICE1: a
668 regulator of cold-induced transcriptome and freezing tolerance in *Arabidopsis*. *Genes &*
669 *Development* 17, 1043–1054.
670 Chinnusamy V., Zhu J. & Zhu J.K. (2007) Cold stress regulation of gene expression in plants.
671 *Trends in Plant Science* 12, 444–451.
672 Davis A.M., Hall A., Millar A.J., Darrah C. & Davis S.J. (2009) Streamlined subprotocols for
673 floral-dip transformation and selection of transformants in *Arabidopsis thaliana. Plant*
674 *Methods* 5, 1–7.
675 Di Laurenzio L., Wysocka-Diller J., Malamy J.E., Pysh L., Helariutta Y., Freshour G., … &
676 Benfey PN (1996) The *SCARECROW* gene regulates an asymmetric cell division that is
677 essential for generating the radial organization of the *Arabidopsis* root. *Cell* 86, 423–433.
678 Ding Y., Li H., Zhang X., Xie Q., Gong Z. & Yang S. (2015) OST1 kinase modulates freezing
679 tolerance by enhancing ICE1 stability in *Arabidopsis*. *Developmental Cell* 3, 278–289.
680 Doherty C.J., Van Buskirk H.A., Myers S.J. & Thomashow M.F. (2009) Roles for *Arabidopsis*
681 CAMTA transcription factors in cold-regulated gene expression and freezing tolerance.
682 *Plant Cell* 21, 972–984.
683 Dubois M., Skirycz A., Claeys H., Maleux K., Dhondt S., De Bodt S., … & Inzé D. (2013)
684 Ethylene Response Factor6 acts as a central regulator of leaf growth under water-limiting
685 conditions in *Arabidopsis*. *Plant Physiology* 162, 319–332.

bioRxiv preprint doi: https://doi.org/10.1101/848705; this version posted November 20, 2019. The copyright holder for this preprint (which was not certified by peer review) is the author/funder, who has granted bioRxiv a license to display the preprint in perpetuity. It is made available under aCC-BY-NC-ND 4.0 International license.

686 Dubois M., Van den Broeck L., Claeys H., Van Vlierberghe K., Matsui M. & Inzé D. (2015) The
687 ETHYLENE RESPONSE FACTORS ERF6 and ERF11 antagonistically regulate mannitol-
688 induced growth inhibition in *Arabidopsis*. *Plant Physiology* 169, 166–179.
689 Edgar R.C. (2004) MUSCLE: multiple sequence alignment with high accuracy and high
690 throughput. *Nucleic Acids Research* 32, 1792–1797.
691 Fujimoto S.Y., Ohta M., Usui A., Shinshi H. & Ohme-Takagi M. (2000) *Arabidopsis* ethylene
692 responsive element binding factors act as transcriptional activators or repressors of GCC
693 box-mediated gene expression. *Plant Cell* 12, 393–404.
694 Fursova O.V., Pogorelko G.V. & Tarasov V.A. (2009) Identification of ICE2, a gene involved in
695 cold acclimation which determines freezing tolerance in *Arabidopsis thaliana*. *Gene* 429,
696 98–103.
697 Hao D., Ohme-Takagi M. & Sarai A. (1998) Unique mode of GCC box recognition by the DNA-
698 binding domain of ethylene-responsive element-binding factor (ERF domain) in plants.
699 *Journal of Biological Chemistry* 273, 26857–26861.
700 Horton P., Park K.J., Obayashi T., Fujita N., Harada H., Adams-Collier C.J.& Nakai K. (2007)
701 WoLF PSORT: protein localization predictor. *Nucleic Acids Research* 35, 585–587.
702 Huala E., Dickerman A.W., Garcia-Hernandez M., Weems D., Reiser L., LaFond F., … & Rhee
703 S.Y. (2001) The *Arabidopsis* Information Resource (TAIR): a comprehensive database and
704 web-based information retrieval, analysis, and visualization system for a model plant.
705 *Nucleic Acids Research* 2, 102–105.
706 Jefferson R.A., Kavanagh T.A. & Bevan M.W. (1987) GUS fusions: beta-glucuronidase as a
707 sensitive and versatile gene fusion marker in higher plants. *The EMBO Journal* 6, 3901–
708 3907.
709 Jeon J., Cho C., Lee M.R., Van Binh N. & Kim J. (2016) CYTOKININ RESPONSE FACTOR2
710 (CRF2) and CRF3 regulate lateral root development in response to cold stress in
711 *Arabidopsis*. *Plant Cell* 28, 1828–1843.

bioRxiv preprint doi: https://doi.org/10.1101/848705; this version posted November 20, 2019. The copyright holder for this preprint (which was not certified by peer review) is the author/funder, who has granted bioRxiv a license to display the preprint in perpetuity. It is made available under aCC-BY-NC-ND 4.0 International license.

712 Jia Y., Ding Y., Shi Y., Zhang X., Gong Z. & Yang S. (2016) The *cbfs* triple mutants reveal the
713 essential functions of CBFs in cold acclimation and allow the definition of CBF regulons in
714 *Arabidopsis. New Phytologist* 212, 345–353.
715 Karimi B., Bleys A., Vanderhaeghen R. & Hilson P. (2007a) Building blocks for plant gene
716 assembly. *Plant Physiology* 145, 1183–1191.
717 Karimi M., De Meyer B. & Hilson P. (2005) Modular cloning in plant cells. *Trends in Plant*
718 *Science* 10, 103–105.
719 Karimi M., Depicker A. & Hilson P. (2007b) Recombinational cloning with plant Gateway
720 vectors. *Plant Physiology* 145, 1144–1154.
721 Kim S.H., Kim H.S., Bahk S., An J., Yoo Y., Kim J.Y. & Chung W.S. (2017) Phosphorylation of
722 the transcriptional repressor MYB15 by mitogen-activated protein kinase 6 is required for
723 freezing tolerance in *Arabidopsis*. *Nucleic Acids Research* 45, 6613–6627.
724 Kim N.Y., Jang Y.J. & Park O.K. (2018) AP2/ERF family transcription factors ORA59 and
725 RAP2.3 interact in the nucleus and function together in ethylene responses. *Frontiers in*
726 *Plant Science* 19, 1675.
727 Kizis D., Lumbreras V. & Pages M. (2001) Role of AP2/EREBP transcription factors in gene
728 regulation during abiotic stress. *FEBS Letters* 498, 187–189.
729 Li H., Ding Y., Shi Y., Zhang X., Zhang S., Gong Z. & Yang S. (2017) MPK3- and MPK6-
730 mediated ICE1 phosphorylation negatively regulates ICE1 stability and freezing tolerance in
731 *Arabidopsis*. *Developmental Cell* 43, 630–642.
732 Lee B., Henderson D.A. & Zhua J. (2005) The Arabidopsis cold-responsive transcriptome and
733 its regulation by ICE1. *Plant Cell* 17, 3155–3175.
734 Licausi F., Ohme-Takagi M. & Perata P. (2013) APETALA2/Ethylene Responsive Factor
735 (AP2/ERF) transcription factors: mediators of stress responses and developmental
736 programs. *New Phytologist* 199, 639–649.

bioRxiv preprint doi: https://doi.org/10.1101/848705; this version posted November 20, 2019. The copyright holder for this preprint (which was not certified by peer review) is the author/funder, who has granted bioRxiv a license to display the preprint in perpetuity. It is made available under aCC-BY-NC-ND 4.0 International license.

737 Liu Q., Kasuga M., Sakuma Y., Abe H., Miura S., Yamaguchi-Shinozaki K. & Shinozaki K.
738 (1998) Two transcription factors, DREB1 and DREB2, with an EREBP/AP2 DNA binding
739 domain separate two cellular signal transduction pathways in drought- and low-
740 temperature-responsive gene expression, respectively, in *Arabidopsis*. *Plant Cell* 10, 1391–
741 1406.

742 Mase K., Ishihama N., Mori H., Takahashi H., Kaminaka H., Kodama M. & Yoshioka H. (2013)
743 Ethylene-responsive AP2/ERF transcription factor MACD1 participates in phytotoxin-
744 triggered programmed cell death. *Molecular Plant Microbe Interaction* 26, 868–879.

745 Meng X., Xu J., He Y., Yang K.Y., Mordorski B., Liu Y. & Zhang S. (2013) Phosphorylation of an
746 ERF transcription factor by *Arabidopsis* MPK3/MPK6 regulates plant defense gene
747 induction and fungal resistance. *Plant Cell* 25, 1126–1142.

748 Miura K., Jin J.B., Lee J., Yoo C.Y., Stirm V., Miura T., … & Hasegawa P.M. (2007) SIZ1-
749 mediated sumoylation of ICE1 controls CBF3/DREB1A expression and freezing tolerance in
750 *Arabidopsis*. *Plant Cell* 19, 1403–1414.

751 Moffat C.S., Ingle R.A., Wathugala D.L., Saunders N.J., Knight H. & Knight M.R. (2012) ERF5
752 and ERF6 play redundant roles as positive regulators of JA/Et-mediated defense against
753 *Botrytis cinerea* in *Arabidopsis*. *PLoS One* 7, e35995.

754 Moore M., Vogel M. & Dietz K. (2014) The acclimation response to high light is initiated within
755 seconds as indicated by upregulation of AP2/ERF transcription factor network in
756 *Arabidopsis thaliana. Plant Signaling & Behaviour* 9, 976479.

757 Motte H., Vanneste S. & Beeckman T. (2019) Molecular and environmental regulation of root
758 development. *Annual Review of Plant Biology* 70, 465–488.

759 Müller M. & Munné-Bosch S. (2015) Ethylene response factors: A key regulatory hub in
760 hormone and stress signaling. *Plant Physiology* 169, 32–41.

761 Murashige T. & Skoog F. (1962) A revised medium for rapid growth and bioassays with tobacco
762 tissue cultures. *Physiologia Plantarum* 15, 473–497.

bioRxiv preprint doi: https://doi.org/10.1101/848705; this version posted November 20, 2019. The copyright holder for this preprint (which was not certified by peer review) is the author/funder, who has granted bioRxiv a license to display the preprint in perpetuity. It is made available under aCC-BY-NC-ND 4.0 International license.

763 Nakano T., Suzuki K., Fujimura T. & Shinshi H. (2006) Genome-wide analysis of the *ERF* gene
764 family in *Arabidopsis* and rice. *Plant Physiology* 140, 411–432.
765 Neter J., Kutner M.H., Nachtsheim C.J. & Wasserman W. (1996) Applied linear statistic models.
766 McGraw-Hill, New York
767 Ohme-Takagi M. & Shinshi H. (1995) Ethylene-inducible DNA binding proteins that interact with
768 an ethylene-responsive element. *Plant Cell* 7, 173–182.
769 Park S., Lee C.M., Doherty C.J., Gilmour S.J., Kim Y. & Thomashow M.F. (2015) Regulation of
770 the *Arabidopsis* CBF regulon by a complex low-temperature regulatory network. *The Plant*
771 *Journal* 82, 193–207.
772 Péret B., De Rybel B., Casimiro I., Benková E., Swarup R., Laplaze L., … & Bennett M.J. (2009)
773 Arabidopsis lateral root development: an emerging story. *Trends in Plant Sciences* 14, 399–
774 408.
775 Riechmann J.L. & Meyerowitz E.M. (1998) The AP2/EREBP family of plant transcription factors.
776 *Biological Chemistry* 379, 6336–6346.
777 Riechmann J.L., Heard J., Martin G., Reuber L., Jiang C., Keddie J., ... & Yu G. (2000)
778 *Arabidopsis* transcription factors: genome-wide comparative analysis among eukaryotes.
779 *Science* 290, 2105–2110.
780 Salvi E, Di Mambro R, Pacifici E., Dello Ioio R., Costantino P., Moubayidin L. & Sabatini S.
781 (2018). SCARECROW and SHORTROOT control the auxin/cytokinin balance necessary for
782 embryonic stem cell niche specification. *Plant Signaling & Behaviour* 13, e1507402.
783 Schwab R., Ossowski S., Riester M., Warthmann N. & Weigel D. (2006) Highly specific gene
784 silencing by artificial microRNAs in *Arabidopsis*. *Plant Cell* 18, 1121–1133.
785 Sewelam N., Kazan K., Thomas-Hall S.R., Kidd B.N., Manners J.M. & Schenk P.M. (2013)
786 Ethylene response factor 6 is a regulator of reactive oxygen species signaling in
787 *Arabidopsis*. *PLoS One* 8, e70289.

bioRxiv preprint doi: https://doi.org/10.1101/848705; this version posted November 20, 2019. The copyright holder for this preprint (which was not certified by peer review) is the author/funder, who has granted bioRxiv a license to display the preprint in perpetuity. It is made available under aCC-BY-NC-ND 4.0 International license.

Son G.H., Wan J., Kim H.J., Nguyen X.C., Chung W.S., Hong J.C. & Stacey G. (2012) Ethylene-responsive element-binding factor 5, ERF5, is involved in chitin-induced innate immunity response. *Molecular Plant-Microbe Interactions* 25, 48–60.

Sparks E.E., Drapek C., Gaudinier A., Li S., Ansariola M., … & Benfey P.N. (2016) Establishment of expression in the SHORTROOT-SCARECROW transcriptional cascade through opposing activities of both activators and repressors. *Developmental Cell* 39, 585–596.

Sparkes I.A., Runions J., Kearns A. & Hawes C. (2006) Rapid, transient expression of fluorescent fusion proteins in tobacco plants and generation of stably transformed plants. *Nature Protocols* 1, 2019–2025.

Srivastava R. & Kumar R. (2019) The expanding roles of APETALA2/Ethylene Responsive Factors and their potential applications in crop improvement. *Briefings in Functional Genomics* 00, 1–15.Steinert J., Schiml S., Fauser F. & Puchta H. (2015) Highly efficient heritable plant genome engineering using Cas9 orthologues from *Streptococcus thermophilus* and *Staphylococcus aureus. Plant Journal* 84, 1295–1305.

Swarup K., Benková E., Swarup R., Casimiro I., Péret B., Yang Y., … & Bennett M.J. (2008) The auxin influx carrier LAX3 promotes lateral root emergence. *Nature Cell Biology* 10, 946–954.

Tamura K., Stecher G., Peterson D., Filipski A. & Kumar S. (2013) MEGA6: Molecular evolutionary genetics analysis version 6.0. Molecular Biology and Evolution 30, 2725–2729.

Thalhammer A., Hincha D.K. & Zuther E. (2014) Measuring freezing tolerance: electrolyte leakage and chlorophyll fluorescence assays. *Methods in Molecular Biology* 1166, 15–24.

Thomashow M.F. (1999) Plant cold acclimation: Freezing tolerance genes and regulatory mechanisms. *Annual Review of Plant Physiology and Plant Molecular Biology* 50, 571–599.

bioRxiv preprint doi: https://doi.org/10.1101/848705; this version posted November 20, 2019. The copyright holder for this preprint (which was not certified by peer review) is the author/funder, who has granted bioRxiv a license to display the preprint in perpetuity. It is made available under aCC-BY-NC-ND 4.0 International license.

812 Vilarrasa-Blasi J., González-García M.P., Frigola D., Fàbregas N., Alexiou K.G., LópezBigas N.,
813 … & Caño-Delgado A.I. (2014) Regulation of plant stem cell quiescence by a
814 brassinosteroid signaling module. *Developmental Cell* 30, 36–47.
815 Vogel J.T., Zarka D.G., Van Buskirk H.A., Fowler S.G. & Thomashow M.F. (2005) Roles of the
816 CBF2 and ZAT12 transcription factors in configuring the low temperature transcriptome of
817 *Arabidopsis*. *The Plant Journal* 41, 195–211.
818 Moore M.O., König K., Pecher P., Alsharafa K., Lee J. & Dietz K.J. (2014) Fast retrograde
819 signaling in response to high light involves metabolite export, MITOGEN-ACTIVATED
820 PROTEIN KINASE6, and AP2/ERF transcription factors in *Arabidopsis. Plant Cell* 26,
821 1151–1165.
822 Wang P., Du Y., Zhao X., Miao Y. & Song C.P. (2013) The MPK6-ERF6-ROS-responsive *cis*-
823 acting Element7/GCC box complex modulates oxidative gene transcription and the
824 oxidative response in *Arabidopsis*. *Plant Physiology* 161, 1392–1408.
825 Warde-Farley D., Donaldson S.L., Comes O., Zuberi K., Badrawi R., Chao P., … & Morris Q
826 (2010) The GeneMANIA prediction server: biological network integration for gene
827 prioritization and predicting gene function. *Nucleic Acids Research* 38, 214–220.
828 Xie Z., Nolan T.M., Jiang H. & Yin Y. (2019) AP2/ERF transcription factor regulatory networks in
829 hormone and abiotic stress responses in *Arabidopsis*. *Frontiers of Plant Science* 10, 228.
830 Xin Z. & Browse J. (2000) Cold comfort farm: the acclimation of plants to freezing temperatures.
831 *Plant Cell & Environment* 23, 893–902.
832 Yamaguchi-Shinozaki K. & Shinozaki K. (2006) Transcriptional regulatory networks in cellular
833 responses and tolerance to dehydration and cold stresses. *Annual Review of Plant Biology*
834 57, 781–803.
835 Zhao C., Zhang Z., Xie S., Si T., Li Y. & Zhu J.K. (2016) Mutational evidence for the critical role
836 of CBF transcription factors in cold acclimation in *Arabidopsis*. *Plant Physiology* 171, 2744–
837 2759.

bioRxiv preprint doi: https://doi.org/10.1101/848705; this version posted November 20, 2019. The copyright holder for this preprint (which was not certified by peer review) is the author/funder, who has granted bioRxiv a license to display the preprint in perpetuity. It is made available under aCC-BY-NC-ND 4.0 International license.

838 Zhao C., Wang P., Si T., Hsu C.C., Wang L., Zayed O., … & Zhu JK. (2017) MAP kinase
839 cascades regulate the cold response by modulating ICE1 protein stability. *Developmental*
840 *Cell* 43, 618–629.
841 Zuther E., Schulz E., Childs L.H. & Hincha DK. (2012) Clinal variation in the non-acclimated and
842 cold-acclimated freezing tolerance of *Arabidopsis thaliana* accessions. *Plant Cell &*
843 *Environment* 35, 1860–1878.
844

bioRxiv preprint doi: https://doi.org/10.1101/848705; this version posted November 20, 2019. The copyright holder for this preprint (which was not certified by peer review) is the author/funder, who has granted bioRxiv a license to display the preprint in perpetuity. It is made available under aCC-BY-NC-ND 4.0 International license.

FIGURE LEGENDS

Figure 1. Description of the ERF102 to ERF105 proteins of *Arabidopsis thaliana*. (a) Structure of the *Arabidopsis* ERF102 to ERF105 proteins. The schematic representation shows the protein structures of ERF102 to ERF105 according to Nakano *et al.* (2006). The striped lines represent the protein sequences, the hexagons indicate the AP2/ERF DNA-binding domain, black lines putative phosphorylation sites, dashed lines the putative transactivation domains (Nakano *et al*., 2006) and grey boxes the nuclear localisation signals determined with WoLF PSORT (Horton *et al.*, 2007). (b) An unrooted phylogenetic tree of group IXb ERF transcription factors showing the close evolutionary relationship between ERF102 to ERF105 (red box) that are studied. The phylogenetic tree was constructed using MEGA6, the numbers indicate bootstrap values (Tamura, Stecher, Peterson, Filpski & Kumar, 2013).

Figure 2. Regulation of ERF102 to ERF105 gene expression. Relative expression of *ERF102* to *ERF105* in eleven-day-old wild-type seedlings (eight pooled seedlings per sample) after hormone or stress treatment. (a) Auxin (10 µM NAA), (b) salicylic acid (10 mM SA), (c) heat (42 °C), (d) high light (1000 µmol m^{-2} s^{-1}), (e and f) oxidative stress (e; 500 mM H_2O_2, f; 30 µM paraquat), (g) drought, (h) salt (200 mM NaCl) and (i) osmotic stress (200 mM mannitol). Transcript levels of wild-type samples under control conditions were set to 1 ($n \geq 4$). Asterisks indicate significant differences to the respective mock treatment (*, $p < 0.05$; **, $p < 0.01$; ***, $p < 0.001$). Error bars represent SE.

Figure 6. Expression of selected cold-responsive genes in lines with reduced *ERF102* to *ERF105* expression. Relative expression of *CBF1* (a), *CBF2* (b), *CBF3* (c), *COR15A* (d), *COR15B* (e) and *ZAT12* (f) genes in lines with reduced *ERF102* to *ERF105* expression before (non-acclimated, NA) and after 14 days (acclimated, ACC14) of cold acclimation at 4 °C.

bioRxiv preprint doi: https://doi.org/10.1101/848705; this version posted November 20, 2019. The copyright holder for this preprint (which was not certified by peer review) is the author/funder, who has granted bioRxiv a license to display the preprint in perpetuity. It is made available under aCC-BY-NC-ND 4.0 International license.

870 Transcript levels of wild-type samples under non-acclimated conditions were set to 1 ($n \geq 4$).
871 Asterisks indicate significant differences to the respective wild-type condition, (*, $p < 0.05$; **,
872 $p < 0.01$; ***, $p < 0.001$). Error bars represent SE.
873
874 **Figure 7. Electrolyte leakage assays of lines with reduced *ERF102* to *ERF105* expression.**
875 Electrolyte leakage assays with detached leaves of lines with mutations or reduced expression
876 affecting single *ERF* genes (a) or several *ERF* genes (b) before (non-acclimated, NA) and after
877 14 days (acclimated, ACC14) of cold acclimation at 4 °C. The bars represent the means ± SE
878 from four replicate measurements where each replicate comprised leaves from three plants.
879 Asterisks indicate significant differences to the wild type (*, $p < 0.05$; **, $p < 0.01$; ***, $p < 0.001$).

bioRxiv preprint doi: https://doi.org/10.1101/848705; this version posted November 20, 2019. The copyright holder for this preprint (which was not certified by peer review) is the author/funder, who has granted bioRxiv a license to display the preprint in perpetuity. It is made available under aCC-BY-NC-ND 4.0 International license.

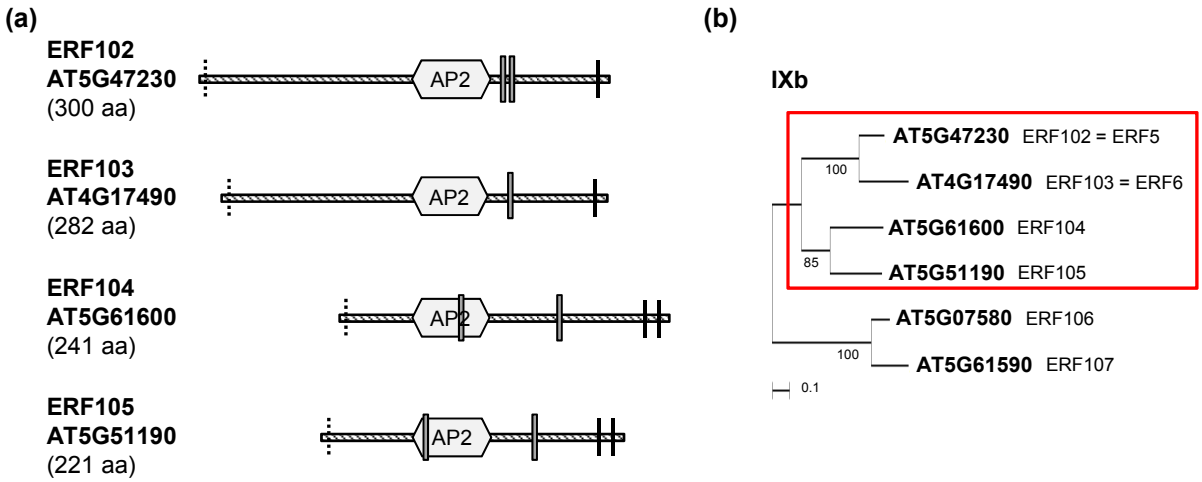

Figure 1. Description of the ERF102 to ERF105 proteins of *Arabidopsis thaliana*. (a) Structure of the *Arabidopsis* ERF102 to ERF105 proteins. The schematic representation shows the protein structures of ERF102 to ERF105 according to Nakano *et al.* (2006). The striped lines represent the protein sequences, the hexagons indicate the AP2/ERF DNA-binding domain, black lines putative phosphorylation sites, dashed lines the putative transactivation domains (Nakano *et al*., 2006) and grey boxes the nuclear localisation signals determined with WoLF PSORT (Horton *et al.*, 2007). (b) An unrooted phylogenetic tree of group IXb ERF transcription factors showing the close evolutionary relationship between ERF102 to ERF105 (red box) that are studied. The phylogenetic tree was constructed using MEGA6, the numbers indicate bootstrap values (Tamura, Stecher, Peterson, Filpski & Kumar, 2013).

bioRxiv preprint doi: https://doi.org/10.1101/848705; this version posted November 20, 2019. The copyright holder for this preprint (which was not certified by peer review) is the author/funder, who has granted bioRxiv a license to display the preprint in perpetuity. It is made available under aCC-BY-NC-ND 4.0 International license.

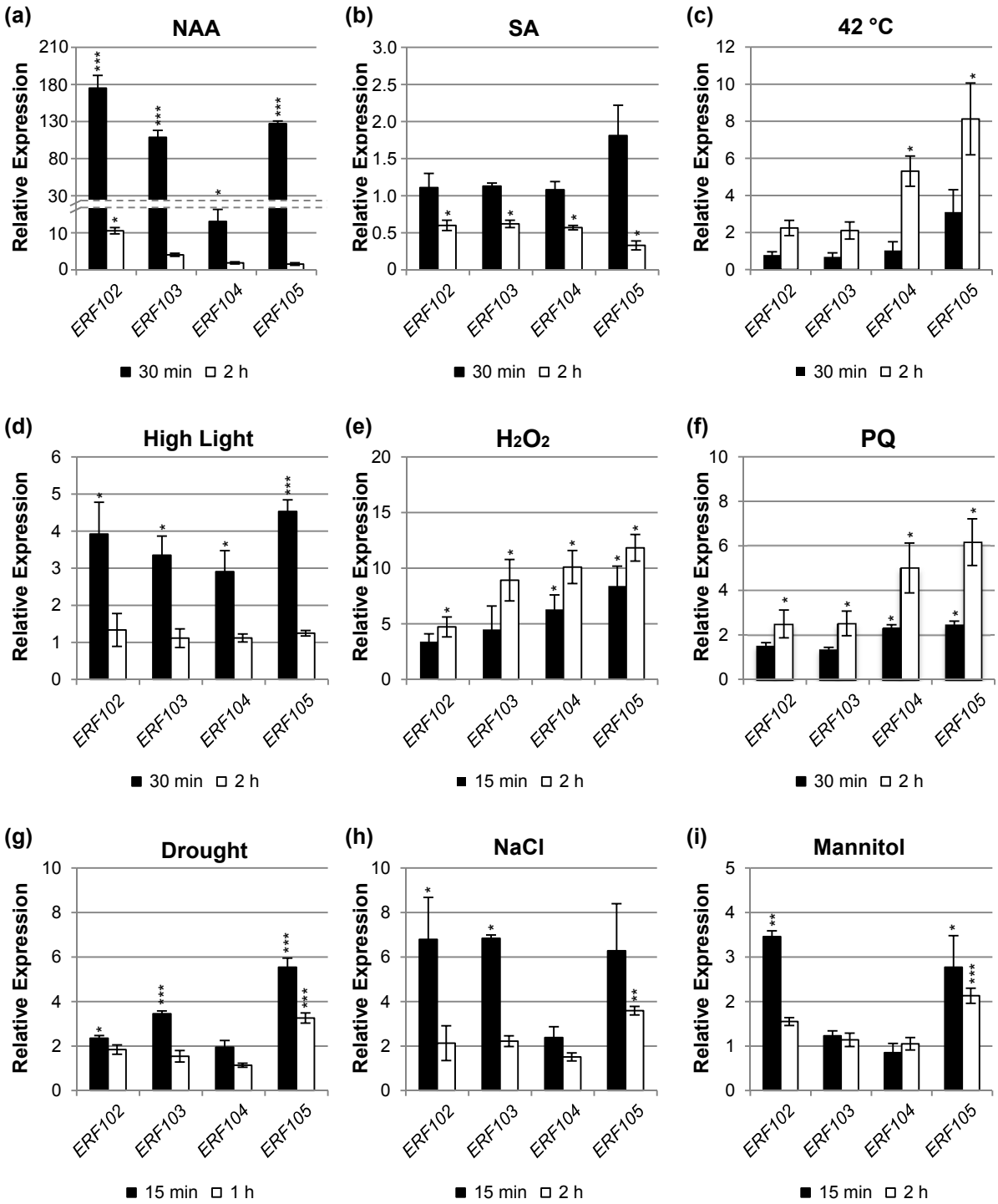

Figure 2. Regulation of *ERF102* to *ERF105* gene expression. Relative expression of *ERF102* to *ERF105* in eleven-day-old wild-type seedlings (eight pooled seedlings per sample) after hormone or stress treatment. (a) Auxin (10 µM NAA), (b) salicylic acid (10 mM SA), (c) heat (42 °C), (d) high light (1000 µmol m^{-2} s^{-1}), (e and f) oxidative stress (e; 500 mM H_2O_2, f; 30 µM paraquat), (g) drought, (h) salt (200 mM NaCl) and (i) osmotic stress (200 mM mannitol). Transcript levels of wild-type samples under control conditions were set to 1 ($n \geq 4$). Asterisks indicate significant differences to the respective mock treatment (*, $p < 0.05$; **, $p < 0.01$; ***, $p < 0.001$). Error bars represent SE.

bioRxiv preprint doi: https://doi.org/10.1101/848705; this version posted November 20, 2019. The copyright holder for this preprint (which was not certified by peer review) is the author/funder, who has granted bioRxiv a license to display the preprint in perpetuity. It is made available under aCC-BY-NC-ND 4.0 International license.

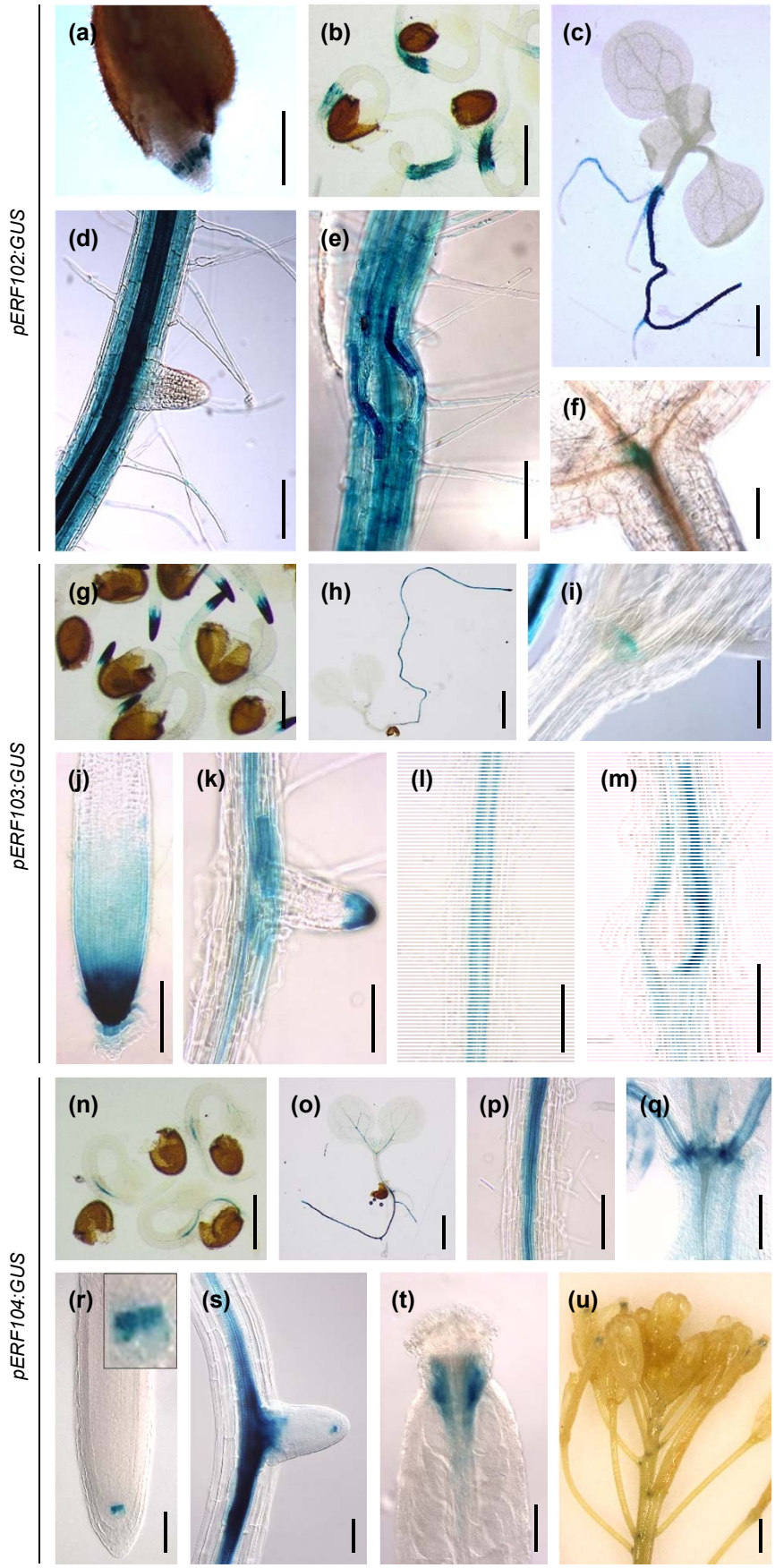

Figure 3. Expression of the *GUS* reporter gene under control of the *ERF102*, *ERF103* and *ERF104* promoters. Histochemical localisation of GUS activity in *Arabidopsis pERF:GUS* reporter lines. *pERF102:GUS* seedlings 30 h (a) and 60 h (b) after imbibition of seeds and ten DAG (c–f). (a) and (b) germinating seeds, (c) whole seedling, (d) and (e) primary root with emerging lateral roots and (f) shoot apex with a stained apical meristem. *pERF103:GUS* seedlings 60 h (g) after imbibition of seeds and seven DAG (h–m). (g) Germinating seeds, (h) whole seedling, (i) shoot apex with

bioRxiv preprint doi: https://doi.org/10.1101/848705; this version posted November 20, 2019. The copyright holder for this preprint (which was not certified by peer review) is the author/funder, who has granted bioRxiv a license to display the preprint in perpetuity. It is made available under aCC-BY-NC-ND 4.0 International license.

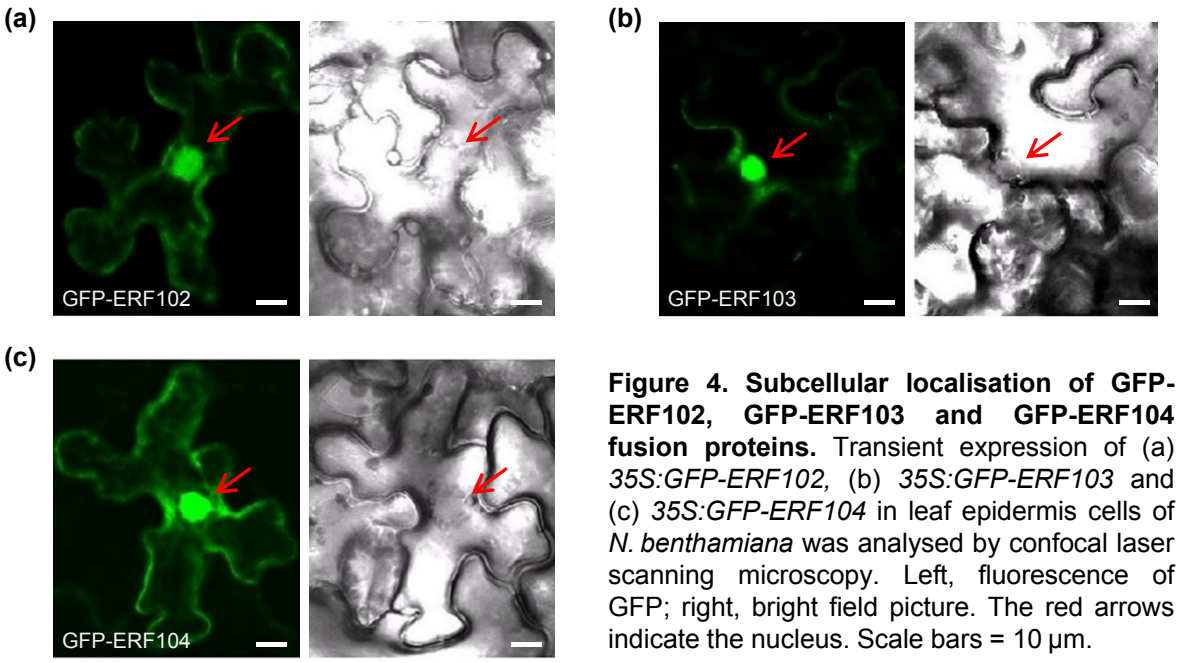

Figure 4. Subcellular localisation of GFP-ERF102, GFP-ERF103 and GFP-ERF104 fusion proteins. Transient expression of (a) *35S:GFP-ERF102,* (b) *35S:GFP-ERF103* and (c) *35S:GFP-ERF104* in leaf epidermis cells of *N. benthamiana* was analysed by confocal laser scanning microscopy. Left, fluorescence of GFP; right, bright field picture. The red arrows indicate the nucleus. Scale bars = 10 µm.

bioRxiv preprint doi: https://doi.org/10.1101/848705; this version posted November 20, 2019. The copyright holder for this preprint (which was not certified by peer review) is the author/funder, who has granted bioRxiv a license to display the preprint in perpetuity. It is made available under aCC-BY-NC-ND 4.0 International license.

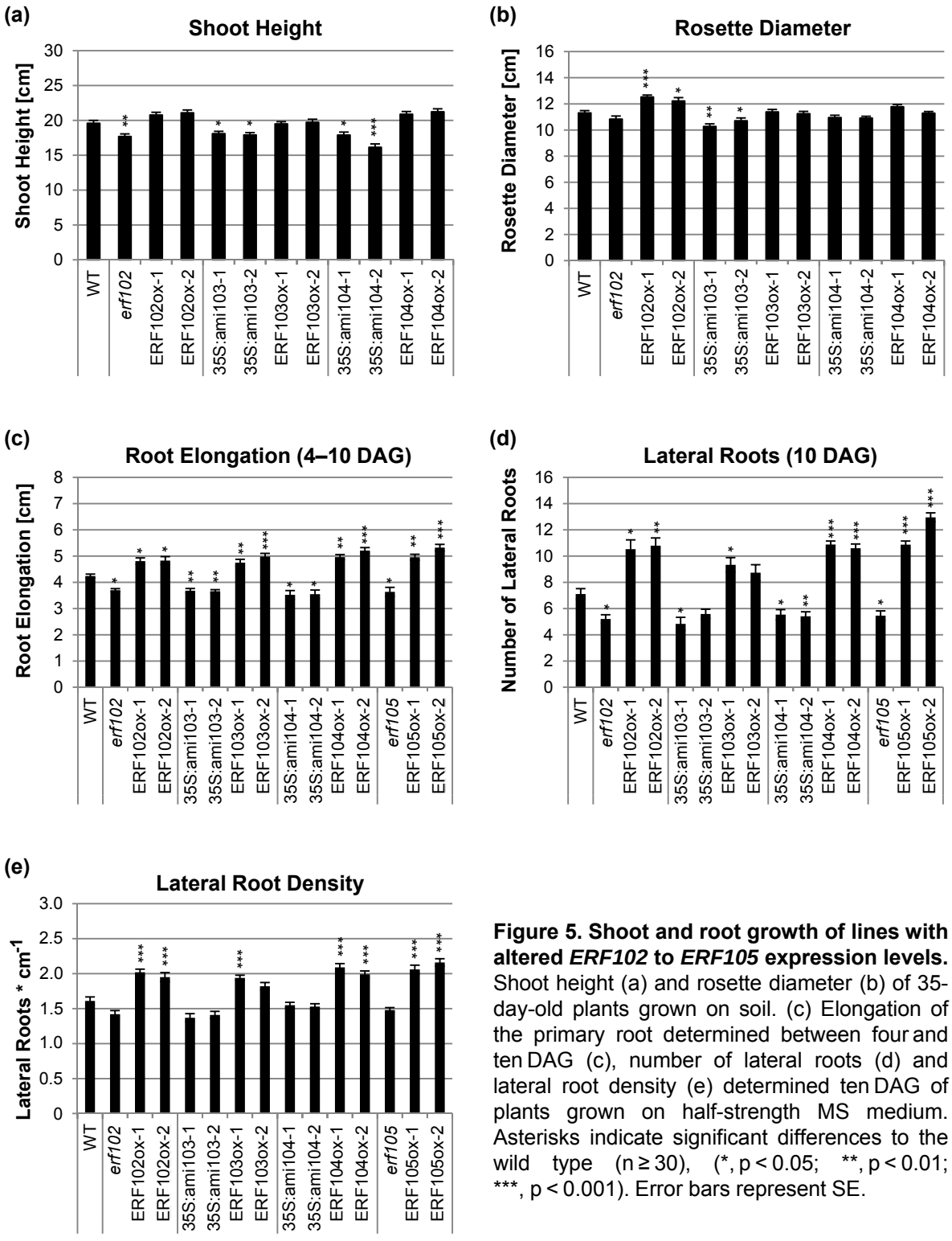

Figure 5. Shoot and root growth of lines with altered *ERF102* to *ERF105* expression levels. Shoot height (a) and rosette diameter (b) of 35-day-old plants grown on soil. (c) Elongation of the primary root determined between four and ten DAG (c), number of lateral roots (d) and lateral root density (e) determined ten DAG of plants grown on half-strength MS medium. Asterisks indicate significant differences to the wild type ($n \geq 30$), (*, $p < 0.05$; **, $p < 0.01$; ***, $p < 0.001$). Error bars represent SE.

bioRxiv preprint doi: https://doi.org/10.1101/848705; this version posted November 20, 2019. The copyright holder for this preprint (which was not certified by peer review) is the author/funder, who has granted bioRxiv a license to display the preprint in perpetuity. It is made available under aCC-BY-NC-ND 4.0 International license.

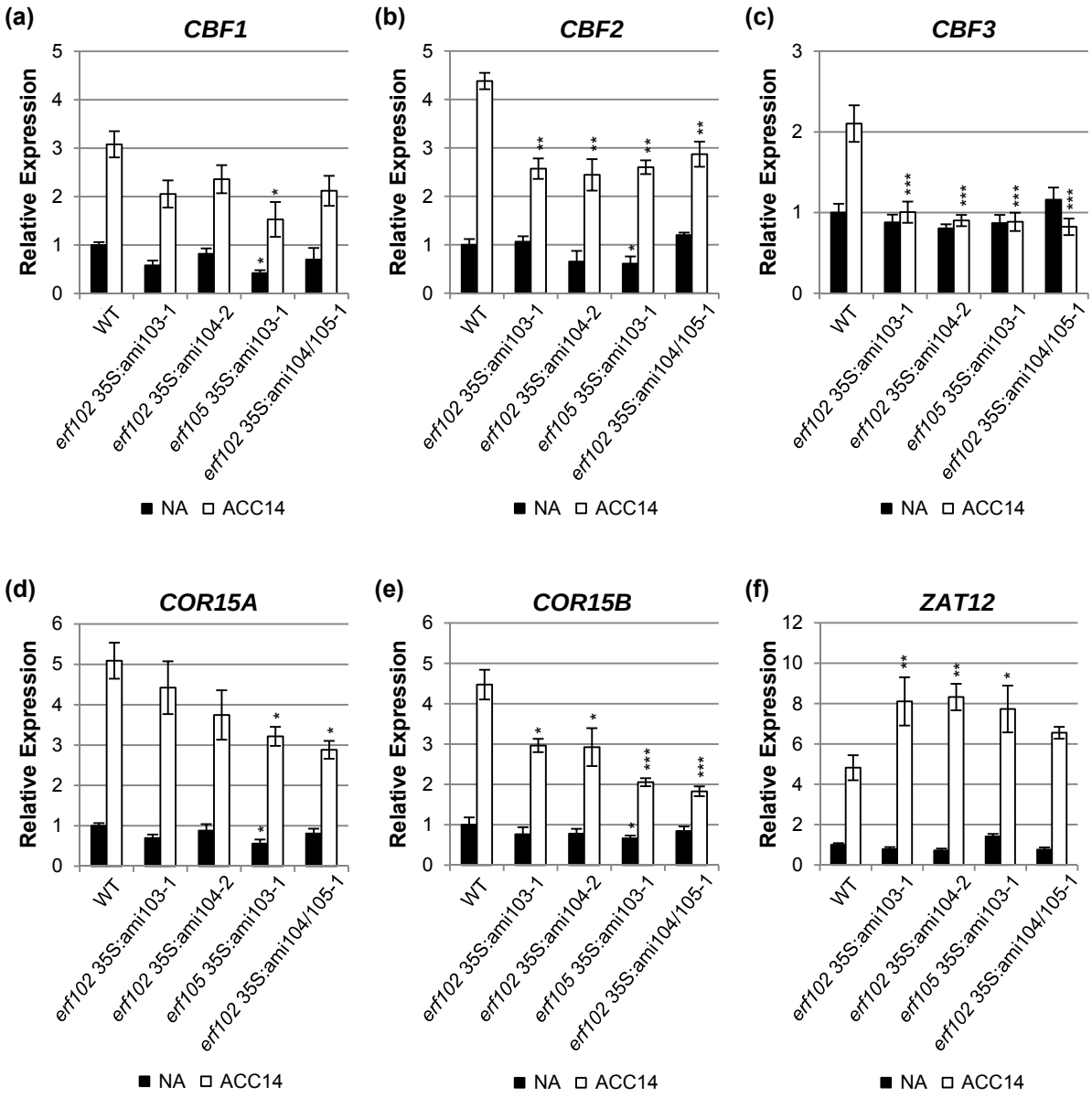

Figure 6. Expression of selected cold-responsive genes in lines with reduced *ERF102* to *ERF105* expression. Relative expression of *CBF1* (a), *CBF2* (b), *CBF3* (c), *COR15A* (d), *COR15B* (e) and *ZAT12* (f) genes in lines with reduced *ERF102* to *ERF105* expression before (non-acclimated, NA) and after 14 days (acclimated, ACC14) of cold acclimation at 4 °C. Transcript levels of wild-type samples under non-acclimated conditions were set to 1 ($n \geq 4$). Asterisks indicate significant differences to the respective wild-type condition (*, $p < 0.05$; **, $p < 0.01$; ***, $p < 0.001$). Error bars represent SE.

bioRxiv preprint doi: https://doi.org/10.1101/848705; this version posted November 20, 2019. The copyright holder for this preprint (which was not certified by peer review) is the author/funder, who has granted bioRxiv a license to display the preprint in perpetuity. It is made available under aCC-BY-NC-ND 4.0 International license.

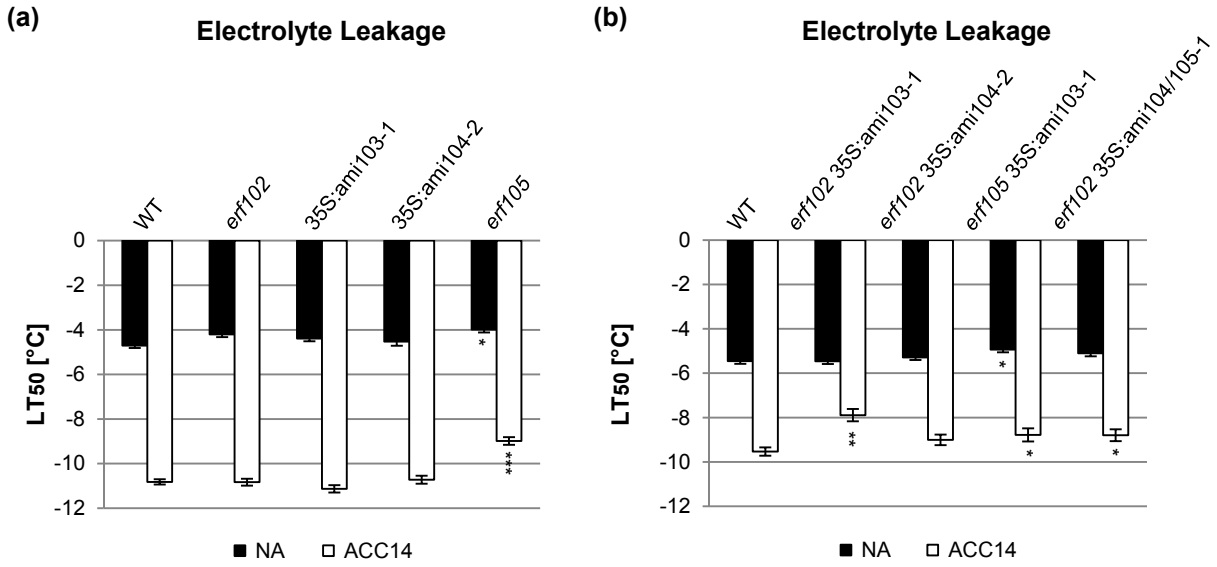

Figure 7. Electrolyte leakage assays of lines with reduced *ERF102* to *ERF105* expression. Electrolyte leakage assays on detached leaves of lines with mutations or reduced expression affecting single *ERF* genes (a) or several *ERF* genes (b) before (non-acclimated, NA) and after 14 days (acclimated, ACC14) of cold acclimation at 4 °C. The bars represent the means ± SE from four replicate measurements where each replicate comprised leaves from three plants. Asterisks indicate significant differences to the wild type (*, $p < 0.05$; **, $p < 0.01$; ***, $p < 0.001$).